

Deliverable D3.8

Laboratory results and methodology to scale-up technologies



Feasible Recovery of critical raw materials through a new circular Ecosystem for a Li-Ion Battery cross-value chain in Europe

WP3 - Recycling technologies and materials re-using for Li-batteries

D3.8 - Laboratory results and methodology to scale-up technologies

Due date of deliverable
31/08/2024

Actual submission date:
30/08/2024

Organisation responsible for this deliverable: CSIC

Dissemination Level

SEN	Sensitive	
PU	Public	X

Project Acronym
FREE4LiB

Project Start Date
01-09-2022

Duration
48 months

Grant Agreement No.
101069890

Project End Date
31-08-2026



Funded by
the European Union

Views and opinions expressed are those of the author(s) only and do not necessarily reflect those of the European Union or CINEA. Neither the European Union nor the granting authority can be held responsible for them. This project has received funding from Horizon Europe research and innovation programme under Grant Agreement No.1069890

@FREE4LiB
 FREE4LiB
 freeforlib.eu

Disclaimer

©2022 FREE4LiB Consortium Partners. All rights reserved.

Free4lib is an EU-funded project that has received funding from the European Union's Horizon Europe research and innovation programme under grant agreement no. 101069890. The sole responsibility for the content of this report lies with the authors. It does not necessarily reflect the opinion of the European Union. The European Commission is not responsible for any use that may be made of the information contained therein.

While this publication has been prepared by the consortium partners of the project, the authors provide no warranty with regards to the content and shall not be liable for any direct, incidental or consequential damages that may result from the use of the information or the data contained therein.

Versions

DATE	VERSION	AUTHOR	COMMENT
16/08/2024	1	ACCUREC, AIMPLAS, CARTIF, CSIC, EURECAT FRAUNHOFER, LUREDERRA, TORRECID,	first draft of the document
30/08/2024	2	CSIC; CARTIF	final document



Contents

Contents	4
1. Executive summary	8
2. Introduction.....	8
3. Dismantling of EOL LIBs supported by robots.....	10
3.1 Results.....	10
3.2 Methodology to scale-up	14
4. Pre-treatment and sorting of Li-ion batteries	16
4.1 Results.....	16
4.2 Methodology to scale-up	28
5. Recycling of black mass.....	30
5.1 Results.....	30
5.2 Methodology to scale-up	38
6. Cathode direct recycling processes	43
6.1 Results.....	43
6.2 Methodology to scale-up	44
7. Recycling of plastics	45
7.1 Results.....	45
7.1.1 Case study #1 Cell pouch frames	48
7.1.2 Case study #2 Pipes and fittings cooling system.....	50
7.1.3 Case study #3 Protective and insulating panels	53
7.2 Methodology to scale-up	56
7.2.1 Case study #1 Cell pouch frames	57
7.2.2 Case study #2 Cooling system tubes.....	58
7.2.3 Case study #3 Protective and insulating panels	60
8. Recycling of metals	62

8.1	Results.....	62
8.1.1	Battery case disassembling and pre-melting of the aluminium alloys recovered.....	62
8.1.2	Metal powder production using Vacuum Induction Melting Inert Gas Atomization.....	64
8.1.3	Powder testing and optimisation for selective laser melting additive manufacturing.....	68
8.1.4	Results in powder production using centrifugal atomization	71
8.2	Methodology to scale-up	72
9.	Synthesis of novel active materials	73
9.1	Synthesis of cathode materials by FSP	73
9.2	Synthesis of cathode materials through solid state and hydrothermal processes	80
9.2.1	Synthesis of active materials by solid state.....	80
9.2.2	Methodology to scale-up	92
10.	Cell manufacturing research	94
11.	Study of recovery materials harnessing in other fields	95
11.1	Results.....	95
11.2	Methodology to scale-up	95
12.	Conclusions	96

List of Abbreviations

ACRONYMS	DESCRIPTION
AA	Atomic Adsorption Spectroscopy
ABS	POLYACRYLONITRILE-BUTADIENE-STYRENE
AM	Additive Manufacturing
BM	Black Mass
DES	Deep-Eutectic Solvent
EDS	Energy Dispersive X-ray Spectroscopy
EOL	End-of-Life
EPDM	Synthetic rubber
EV	Electric Vehicle
FSP	Flame Spray Pyrolysis
FTIR	Fourier Transform Infrared spectroscopy
HDPE	High Density Polyethylene
HRC	Human-Robot Collaboration
LIB	Lithium-ion batteries
NIR	Near Infra-Red
PA	Polyamide
PP	Polypropylene
PPE	Polyphenylene Ether
PSDs	Particle Size Distributions
rPA	Recycled Polyamide
rPP	Recycled Polypropylene
rPPE	Recycled Polyphenylene Ether
SEM	Scanning Electron Microscopy

SLM	Selective Laser Melting
TRL	Technology Readiness Level
VIGA	Vacuum Induction Melting Inert Gas Atomisation
XRD	X-Ray Diffraction



1. Executive summary

This deliverable collects the results obtained at lab-scale of the 6 new sustainable and efficient processes to recycle end-of-life (EOL) lithium-ion batteries (LIBs) developed during WP3:

- dismantling
- pre-treatment
- 4 materials recovery processes:
 - cathode direct recycling
 - plastics recycling
 - metals recycling
 - black mass recycling

By analysing the results, at least 6 technologies will be validated at pilot-scale during WP4, and the methodology for each one is described in the deliverable.

2. Introduction

FREE4LIB aims to develop at TRL 5-6 technologies to achieve 6 new sustainable and efficient processes to recycle end-of-life (EOL) LIBs (dismantling, pre-treatment and 4 materials recovery processes) delivering very innovative recycling solutions to reach highly efficient materials recovery (metal oxides, metals and polymers) improving the supply of secondary resources at EU level. FREE4LIB also will deliver technologies to improve 3 processes aiming at metals and polymers re-using and electrode synthesis on the same value chain as secondary raw materials for re-manufacturing greener batteries, and it will study options to harness non-reusable elements in other fields. FREE4LIB will also deliver a methodology based on the Battery Passport principles to improve processes traceability.

Within scope of the project, the WP3 focuses on development of material technology for recovery of valuable materials and their valorisation within the battery value chain.

Nowadays, it is increasingly common to encounter devices powered by lithium batteries. As these batteries reach the end of their lifecycle, environmentally efficient recycling strategies are necessary. The robotic disassembly of electric vehicle (EV) batteries presents significant challenges due to the lack of standardisation in the mechanical and structural design of the batteries. Each EV battery is unique, even among different battery packs from the same manufacturer, making it difficult to develop robots that can disassemble any type of battery. Additionally, EV batteries contain a high energy charge, posing

safety risks during handling, such as potential fires or explosions if not managed properly.

The development of this type of technology with robots represents an opportunity to improve resource management by increasing efficiency, reducing environmental impact, and enhancing safety. Robots can adapt to different designs and conditions of the batteries, achieving precise and safe disassembly. This document details the initial results obtained from investigating the process of disassembling EV batteries with robots and the solutions being prepared at the laboratory level that could be implemented in the industry.

The goal of T3.2 pre-treatment and sorting of disassembled LIBs was implementing 3 different technologies (mechanical separation, electrohydraulic fragmentation, non-breaking delamination) and sorting cells based on Battery Pasion concept. The way to reduce EOL LIBs particle size from modules to electrode foils, black mass, cathode powder, metals and polymers by breaking and non-breaking processes of batteries at lab-scale in view of scaling is carried out and optimized.

Regarding black mass recycling, the lab-scale tests made during T3.3 leads to the definition of a combined pyro-hydrometallurgical process, that allows the preparation of precursors adequate to synthesize active cathode materials, as well as recycled graphite that might be used as active anode materials. These results are here summarized, and the methodology to scale-up this combined process is also collected.

WP3 has focused mainly on recovery within active materials like NMC622 and LMNO. Present deliverable D3.8 shows experimental results achieved within the use of recycled black mass from delamination process and metal precursor mixture obtained, for the synthesis of active materials NMC622 and LNMO, by cost effective, easily scalable technologies. Starting from the results, D3.8 sets guidelines for WP4 focusing on scaling up of revalorization use in active material synthesis

Concerning the production of novel cathode materials from recycled precursors, LUREDERRA and TORRECID are working in their specific technologies, in order to achieve cathodes with good electrochemical performance. In this phase of laboratory scale, they have produced several batches and tested to get feedback and be able to optimised each process depending on the requirements. On *Section 9*. principal results from both technologies as well as main activities done have been summarized. Additionally, the methodology to be followed for the up-scaling has been detailed for both cases.

The increasing adoption of EVs will boost the need for proper recovery of plastic components from EoL vehicles (including interior and battery packs). Some common plastic found in EVs include: battery housings, module casings, connectors, tubes, pipes, charging port covers, etc. Managing these plastic components presents challenges and opportunities given the diverse range of plastics used in vehicle manufacturing. Nevertheless, effective management of these materials is crucial to reduce environmental impact, conserve resources, and promote sustainability in the automotive industry.

The current report summarizes main outcomes related to *Task 3.5 Recycling of plastics at lab-scale* and outlines the results included in deliverable *D3.4 Report on plastic materials recovered and properties characterization*.

Several technologies have been explored during these first 24 months of the project and their scaling up process is key to achieving quality and assurance results at the end of the project in WP4 at a higher TRL 5-6.

The laboratory scale results have been described in the previous deliverables of WP3 and their promising results represent an affordable opportunity to continue investigating these technologies in the following years.

The following sections are structured on the basis of the results obtained at laboratory scale and the methodology proposed for their scale-up or the constraints identified for their non-scale-up.

3. Dismantling of EOL LIBs supported by robots

3.1 Results

The task's objective is to develop a robot-supported battery disassembly line to help recover valuable materials, such as metal oxides, plastics, and metals.

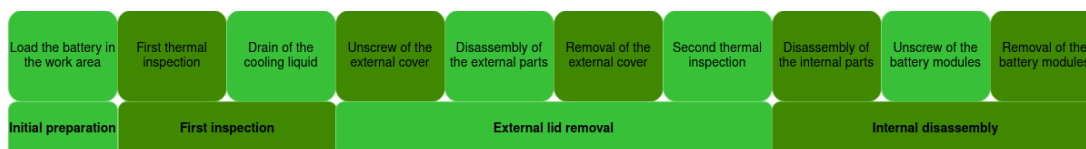
The first phase of the process for dismantling EOL LIBs supported by robots involved in detail analyzing the manual dismantling process to identify opportunities for robotic automation. During the manual disassembly, the tools needed for each task were listed to determine whether a robot could handle them. Manual execution times for each phase were recorded, and the level of risk faced by the operator during these tasks was also documented (Table 1).

Table 1. Manual disassembly process task details

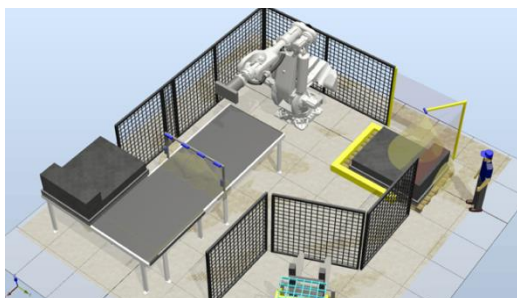
TASK	TIME	TOOLS	RISKS	VOLTAGE	COSTS	POTENTIAL
Backpack the battery	2	Power tools	Low	High	Low	Low
Load the battery	2	Crane	Low	High	Mid	Low
Drain the liquid	1	Air compressor	Low	High	Low	Low
Measure voltage	1	Multimeter	Low	High	Low	Low
Remove the lid	10	Power tools	Low	High	Mid	High
Beddings	2	Hand tools	Low	High	Low	High
Monitor	2	Multimeter	Low	High	Low	Low
Disconnect terminal	15	Hand tools	Low	High	Mid	High
Disconnect	10	Hand tools and	High	Low	Mid	Mid
Electrical cables	10	Hand tools	Puncture	Low	Mid	Mid
Remove the battery from the case	20	Power tools	Puncture	Low	Mid	Low

With all the phases detailed, Eurecat robotics group clustered the tasks based on their potential for automation, focusing on those where precision, speed, and weight handling were critical. The identified stages of the dismantling process included initial battery preparation, inspection, external components extraction, and internal disassembly.

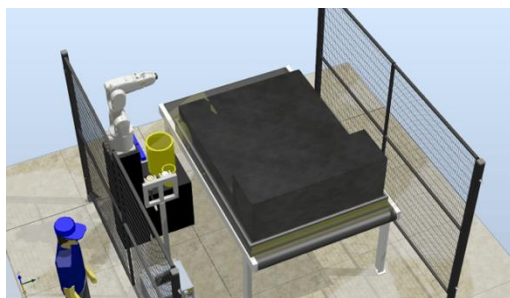
Diagram of the identified robot tasks



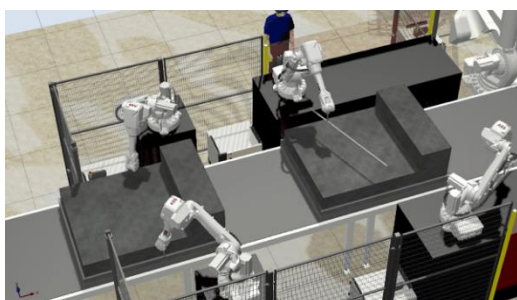
For each identified opportunity for robotic automation, a simulation was designed to validate that the spaces, robots, and tools could effectively execute each task. These simulations allowed for verification of compatibility and efficiency of the robotic systems in a controlled environment.



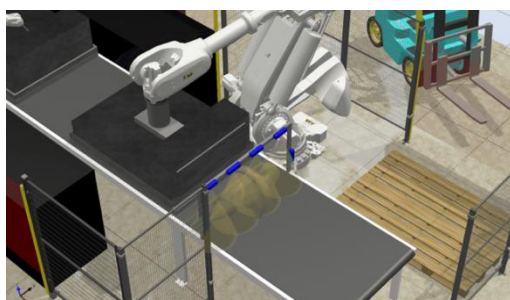
Simulation 1. Load the battery in the work area and first thermal inspection.



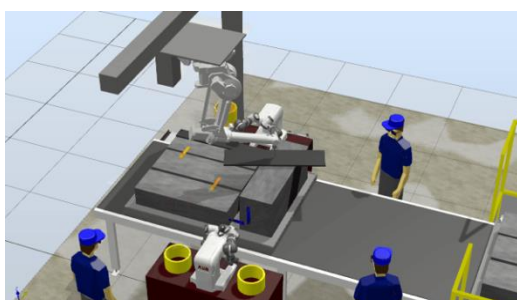
Simulation 2. Remove the cooling liquid.



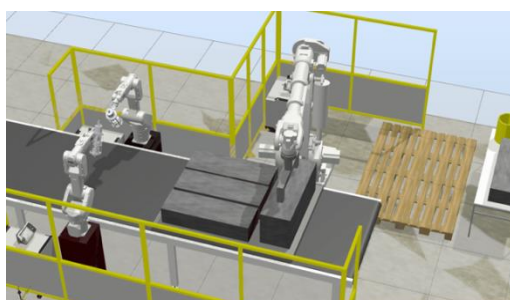
Simulation 3. Remove the external components and unscrew.



Simulation 4. Remove the external lid.



Simulation 5. Remove internal parts and unscrew.



Simulation 6. Battery packs modules manipulation.

After analyzing the different phases, all the information was available to select two tasks to be automated by robots. The tasks selected were the unscrewing of bolts, both external and internal, and the removal of the external battery cover. These tasks were chosen due to the high precision and repeatability required, as well as the risks associated with manually handling heavy and potentially hazardous components.

The reasons for selecting these tasks include improved precision and speed, reduced risks for operators, and optimization of robotic tools' use. Automating these tasks is expected to significantly enhance efficiency and safety compared to the manual process. Manually removing the lid takes about 10 minutes, including unscrewing 20 bolts and manipulating the cover. By automating this process, we anticipate a 15% reduction in time, lowering it to approximately 8.5 minutes. This is based on the robotic process of unscrewing each bolt, which consists of moving the robot to position, unscrewing, and moving to the

position to leave the screw, totaling 8 seconds per bolt, or roughly 2.7 minutes for 20 bolts.

Similarly, removing the internal screws, which currently takes about 15 minutes manually, is expected to be completed in about 10 minutes with robotic automation. Additionally, reducing the number of false unscrewing attempts by 20% can decrease errors, leading to smoother operations. Automating the lid removal will also eliminate the risk of operator injuries during this stage, enhancing safety by 100%. These improvements underscore the significant benefits of integrating robotics into the dismantling process, resulting in higher efficiency and enhanced worker safety.

We trained a model using YOLO (You Only Look Once) to identify screws, achieving a remarkable 95% accuracy in detecting battery screws. This advancement significantly enhances our robotic system's precision in locating and handling these components, ensuring more reliable and efficient automation in the dismantling process.

Image: Screw detection achieved training the model using YOLO.



Finally, a comprehensive validation of the proposed tasks for robotization was conducted, considering various factors. System testing involved extensive trials in a controlled laboratory environment to demonstrate the potential use of

robots in supporting the disassembly process, including sorting input batteries to gather information on their life, charge, criticality, and health. The collaboration between robots and human operators was evaluated, emphasizing the importance of training operators due to the associated risks. The adaptability analysis highlighted the system's ability to accept various types of battery packs and modules, ensuring operation with different modules without constant adjustment of robot parameters. Safety assessments considered the risks related to batteries and human-robot collaboration, implementing strict process controls to avoid shocks, vibrations, temperature, or pressure drops that could cause fires or explosions, and establishing a separate space for storing and checking abnormal batteries. The scale-up potential was assessed by identifying safeguards to separate the disassembly line from other plant operations, utilizing automated disassembly to increase efficiency and speed up the recovery of valuable components, and determining that industrial scale-up would only be feasible if economically viable.

3.2 Methodology to scale-up

The objective of scaling up the robotic dismantling technology is to verify that the automated processes meet the expected performance results and are ready for industrial application. This involves transitioning from laboratory-scale development (TRL 3-4) to pilot-scale validation (TRL 5-6).

The first step involves preparing Eurecat's laboratories to accommodate and test the robotic automation phases. This preparation includes sourcing and acquiring necessary robotics equipment, such as specialized tools for unscrewing bolts and manipulating components. The workspace has been adapted to fit the robotic systems and ensure a safe and efficient testing environment.

To support the robotic dismantling process, Eurecat has procured essential robotic tools and equipment, including robotic arms capable of handling precise and repetitive tasks such as unscrewing bolts and specialized tools for both external and internal screw removal. The workspace has been adapted to integrate these robotic systems seamlessly.

Once the equipment is set up, the next step is programming the robotic systems for the specific tasks of unscrewing external and internal screws and manipulating the external lid. This involves developing and refining algorithms to control the robots' movements, ensure accurate execution of tasks, and integrate safety protocols.

To validate the effectiveness of the robotic systems and ensure they meet the expected performance standards, we will conduct a series of experiments:

- **Performance testing:** Assess the efficiency of robotic systems in unscrewing both external and internal screws compared to manual processes. Metrics will include time reduction, precision improvements, and error rates.
- **Lid manipulation tests:** Evaluate the effectiveness and speed of the robotic system in handling and removing the external battery lid. This will include measuring time savings and the quality of lid removal.
- **Safety assessments:** Conduct tests to ensure that the robotic systems operate safely, minimizing risks of accidents or damage to components. This includes verifying the effectiveness of safety measures and emergency protocols.



Image. Robot with the unscrew hardware

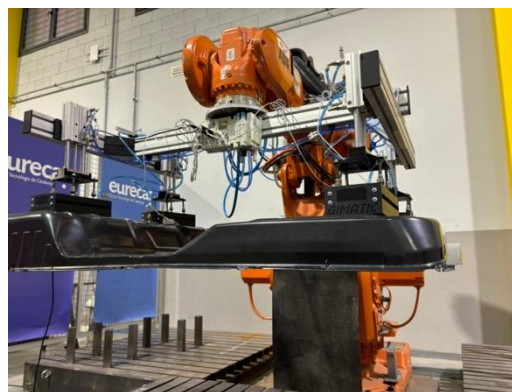


Image. Robot with the manipulation of the lid hardware.

These experiments aim to confirm that the robotic systems can handle the tasks with improved efficiency, precision, and safety. Success in these trials will validate the transition from laboratory-scale testing to pilot-scale implementation, paving the way for industrial-scale applications and commercialization.

The development of these robotic stages is part of Task T4.1, which builds upon the work done in Work Package 3. In the future, Eurecat will focus on refining and scaling the various robotized stages to validate that robots can effectively perform these tasks. By following this methodology, Eurecat aims to advance the robotic dismantling technology to TRL 5-6, demonstrating its readiness for broader deployment in battery recycling operations.

4. Pre-treatment and sorting of Li-ion batteries

4.1 Results

ACCUREC has received batteries packs from RECYCLIA and modules from ERION (Figure 1). Then the material available in these packs, especially those non-cell components at pack and module level has been investigated. Those parts were sent to project partners for further recycling investigation. Besides that, ACCUREC has performed a thermal pre-treatment and mechanical pre-treatment of cells within these packs and modules. Different types of black mass were obtained and the black mass was also sent to project partner for further refinery investigation.





Figure 1. Hyundai Kona battery internal structure (l); Volkswagen module dismantling (r).

After dismantling of battery packs from Recyclia and Erion, Accurec has performed a recycling process to obtain the black mass from cells (Figure 2). The 1st step of recycling process is pyrolysis which batteries will be heated up to 500 °C under vacuum. The goal of pyrolysis is to remove electrolyte and decompose organic plastics in the cells. So that the subsequent mechanical separation is safe. The processing parameters such as heater temperature, chamber temperature, battery temperature and chamber pressure were recorded during the process. It can be found that when pyrolyzing the Hyundai Kona batteries, due to the remaining electric energy, the cells have experienced a thermal run-away event. The temperature of cells has increased from 100 °C to 400 °C in a few seconds. On the other hand, the VW modules are pyrolyzed smoothly without thermal run-away event. The temperature of cells increased gently by the heater from room temperature to 450 °C. Although the heating condition program is set to be the same for both materials, the behavior of batteries in the furnace is completely different.

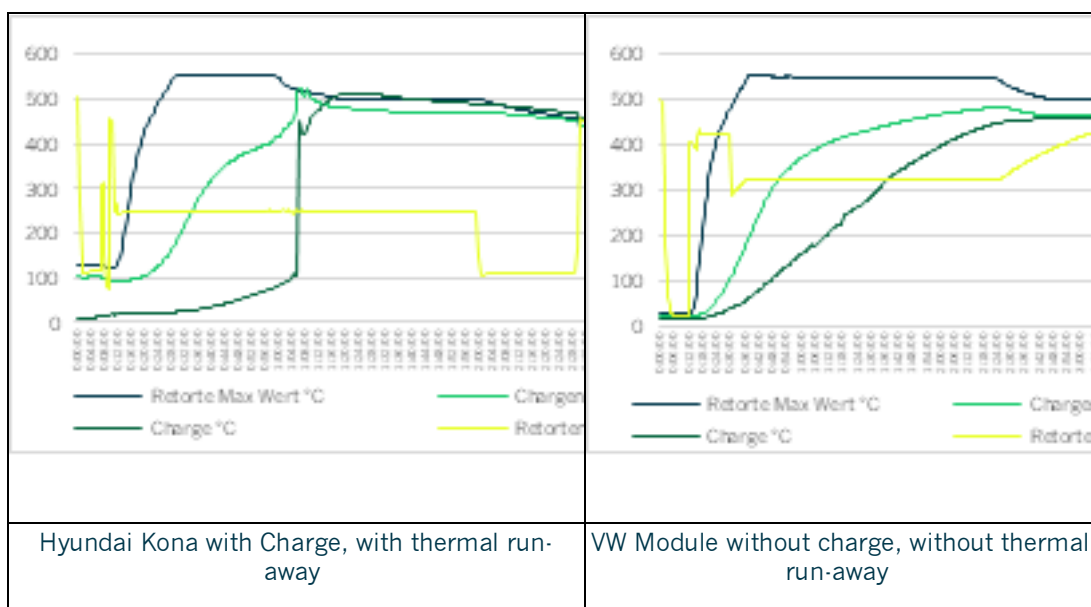


Figure 2. Pyrolysis parameters for both Hyundai Kona and VW modules.

Besides, ACCUREC has also carried out investigation on the quality of black mass. An XRF analysis has been carried out and the results are listed below (Table 2). The metal content in black mass from Hyundai Kona is similar to ACCUREC standard quality of black mass while the metal content in black mass from VW modules are very low. On the other hand, this black mass is mainly composed of carbon. The reason for this difference is mainly due to the charging state of cells during the pyrolysis. The VW cells are fully discharged and have not exceed 500 °C for the whole process. This leads to the incomplete decomposition of the PVDF (binder) between the cathode material and aluminium foils. As a result, part of the cathode material remains in the Al foil and not fall into the category of black mass. Therefore, the quality of black mass from VW is not good enough for the further treatment.

Table 2. XRF analysis of black mass from Hyundai Kona and VW modules.

Element	Kona	VW
Ni	23.8 wt.%	5.74%
Mn	9.49 wt.%	2.89 wt.%
Co	8.3 wt.%	2.21 wt.%
C	42 wt.%	85 wt.%

The activities of FRAUNHOFER in this subtask were focused on the development of the Hydro-mechanical process for highly material-selective comminution and separation by electrohydraulic fragmentation (Figure 3). At the end of the process three fractions (metals, polymers, black mass) were gained. Following the manual dismantling of the battery modules, the exposed cells were placed

in the electro-hydraulic shredding system for further treatment. This special shredding process uses mechanical shock waves, which are generated in a liquid medium (here tap water) to cause the material to be shredded. The aim of these method is the dismantling and separation of the different battery cell types into individual material fractions (plastics, metals, black mass). Following the EHF comminution, the resulting mixed material fractions are separated from each other and concentrated using the skimming and sieving process (SuSi) with regard to their different material properties. Skimming and sieving are primarily about obtaining black matter. The cleaned black mass should be separated from the remaining material such as housing, anode foil, cathode foil, separator foil and plastic materials.

The aim of these method is the dismantling and separation of the different battery cell types into individual material fractions (plastics, metals, black mass). The process parameters of the EHF were chosen to be identical in all tests for reasons of comparison.

- Number of cells: 2 (pouch)
- Reactor size: 30 l
- Amount of water in the reactor: approx. 20 l
- Working voltage: 30-40 kV
- Frequency: 1.5 Hz





Figure 3. EHF process with punch cells.

Following the EHF comminution, the resulting mixed material fractions are separated from each other and concentrated using the skimming and sieving process (SuSi) with regard to their different material properties. SuSi is a prototype of an in-house development by the IWKS. SuSi is a device for sieving and skimming crushed material fractions. The advantage of this process in battery recycling lies in the further treatment of the material when it is wet. This minimizes dust formation in the recycling process, which can release harmful substances into the environment. After skimming and sieving process, the received material fractions are highly pure but wet. The last step of this post-treatment is drying the three fractions in an oven by ca. 60 °C for around 24 hours.

The fine sieve fractions after skimming and sieving step were analysed using ICP-OES to determine the quantitative elemental composition (Table 3). This primarily concerns the black matter fractions and the determination of copper and aluminium impurities. In this way, the quality of the separation of black mass and films can be determined using the EHZ and sieving process. What can be clearly seen in the measurement results is that samples with less process time (what means less received pulses) show significantly lower impurities of aluminium, copper from shredded electrode foils. Towards the selected working voltage, there is no noticeable trend. Even the previous removal of the cell casing only has a small impact on the quality of the black mass. If you look purely at the proportion of the valuable elements' cobalt, manganese and nickel in the black mass, an enrichment can also be seen in the samples with higher processing time. Contamination caused by system abrasion especially iron and to a small extent titanium are negligible.

Table 3. ICP-OES results of black mass from EHF.

Sample Nr.	Al (wt%)	Co (wt%)	Cu (wt%)	Fe (wt%)	Li (wt%)	Mn (wt%)	Ni (wt%)	Ti (wt%)
01Aa	0,954	4,30	1,22	0,0191	2,43	4,06	13,4	0,0126
01Ba	2,66	6,28	2,75	0,0408	3,37	5,99	17,9	0,00645
02a	1,82	5,42	2,27	0,0491	2,94	5,24	15,4	0,00758
03Aa	0,914	2,84	1,47	0,0100	1,62	2,58	8,9	0,00200
03Ba	1,67	7,70	2,22	0,0235	3,72	7,34	23,6	0,00226
04a	1,84	6,79	2,23	0,0184	2,86	6,48	21,2	0,00440
05Aa	1,65	2,74	1,19	0,0156	1,46	2,50	8,8	0,00481
05Ba	2,77	7,48	4,02	0,0739	3,31	6,78	23,4	0,00287
06Aa	1,09	2,87	1,34	0,0079	1,50	2,57	8,68	0,00340

06Ba	3,06	5,84	3,17	0,0479	3,30	6,59	21,9	0,00287
07a	1,78	8,30	3,24	0,0394	4,02	7,73	25,5	0,00226
08a	2,03	5,84	2,82	0,0231	2,61	5,48	18,0	0,00232

In order to investigate where and in what form the impurities are present, SEM images and EDX mappings of the recovered black mass were created (Figure 4). The examined samples were selected based on their different processing. The focus of the evaluation focus was based on comparing black mass taken out of the process early and late. As expected, the degree of comminution and thus the destruction of the particle structure increases with increasing pulse number. This becomes clear in the distribution and shape of the individual particles. This circumstance is particularly important if further recycling in the sense of direct use is planned for the recovered black mass. In particular it becomes clearer when looking at the particle size distribution of the two samples. With fewer pulses, larger and more circular active material particles can be detected, whereas with more pulses the tendency is towards smaller and widely scattered particle fragments.

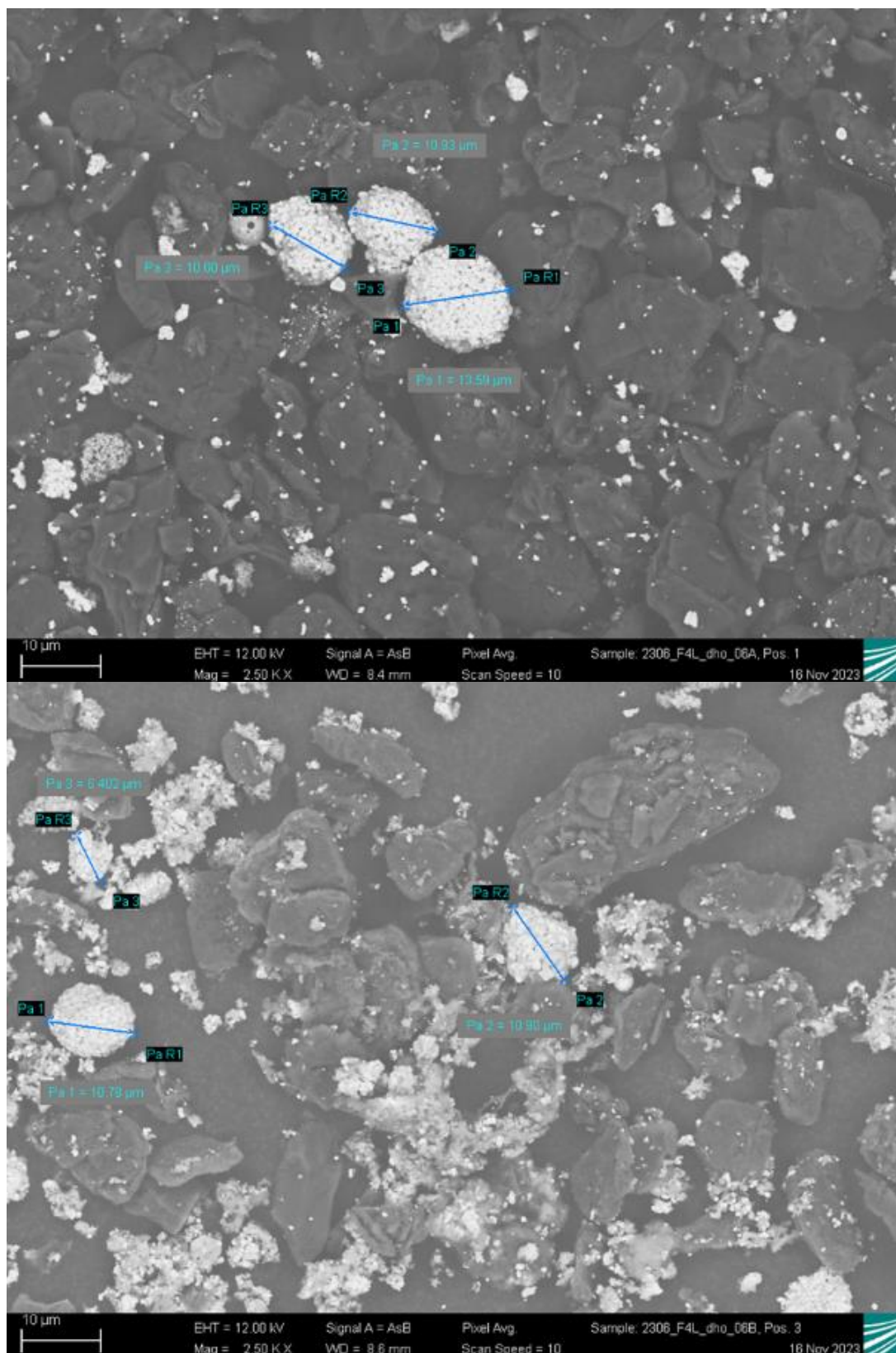
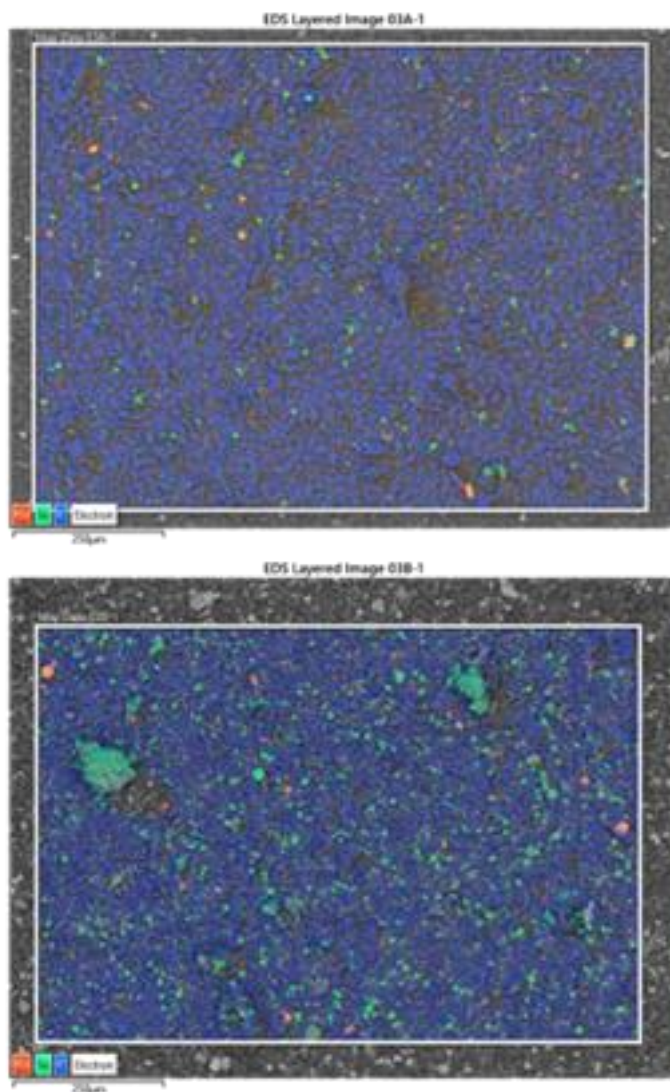


Figure 4. Particle size distribution of EHF black mass.

Both the results from the ICP OES and the previous chapter are confirmed by the created EDX mappings (Figure 5). In the overview at the lower magnification level, you can see significantly fewer distributed active material particles (displayed as Ni) with a short process time. The occurrence of contamination (displayed as Cu) also increases with longer process times. This becomes even clearer in the higher magnification picture.



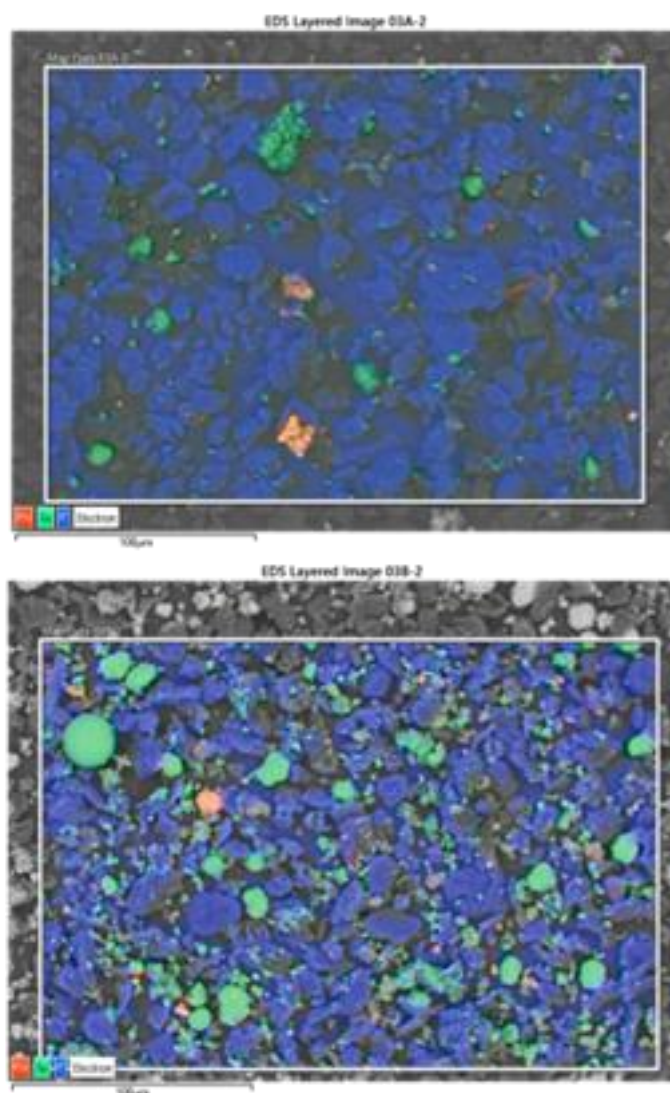


Figure 5. EDX mappings of black mass samples with 250x (top) and 1000x (bottom) magnification.

The aim of the ultrasonic delamination process is to detach the CAM from the cathode aluminium foil and the graphite from the anode copper foil by using high intensity ultrasound. The cavitation from the ultrasonic pulses separates the active material from the current collectors wetted by a liquid solvent.

Table 4. Metal content of the solid CAM recovered after ultrasonication delamination.

Solvent	Concentration (M)	CAM recovery efficiency (%)			
		Co	Li	Mn	Ni
NaOH	0.05	98.28	97.64	76.39	89.72
	0.1	100.00	98.95	75.61	87.48
Oxalic Ac.	0.05	20.55	43.52	25.40	50.20
	0.1	29.51	37.52	25.09	44.70
Citric Ac.	0.05	96.95	98.42	96.17	95.77

	0.1	96.52	100.00	77.07	94.78
--	-----	-------	--------	-------	-------

Table 5. Metal content of the filtrate after ultrasonication delamination.

Solvent	Concentration (M)	Filtrate metals content (mg/L)				
		Co	Li	Mn	Ni	Al
NaOH	0.05	0.00	32.93	0.00	0.00	86.20
	0.1	0.00	36.99	0.00	3.43	183.16
Oxalic Ac.	0.05	24.86	105.07	64.63	606.47	47.77
	0.1	40.52	125.30	149.04	596.29	78.23
Citric Ac.	0.05	0.00	72.09	19.94	270.66	48.68
	0.1	20.97	87.77	78.28	401.10	54.12

In terms of separation efficiency, the Oxalic Acid shows the best results and sodium hydroxide the worst. However, this only refers to the solid fraction in weight average but it should be needed to analysed the metal content of both solid fraction and filtrate after the solid-liquid separation step (Table 4 and Table 5). On the other hand, it should be pointed out that the increase in solvent concentration did not imply a better material separation efficiency, as the results showed. This could be due to its lixiviation power, so that the metal content could have migrated to the liquid phase. ICP-OES analysis has been implemented to understand the metal content in each phase and material recovery efficiency of each metal element. Leaching process was assumed to be the driving force of metal ions from the solid to the liquid phase during the ultrasonication delamination. The highest recovery efficiency in terms of metal elements does not correlate with the results about separation efficiency. Oxalic acid achieved the highest separation efficiency in terms of CAM detachment from the aluminium foil, however, the leaching efficiency was higher in contrast to citric acid, as is shown in the filtrate side. So, metal ions were dissolved in the liquid and it reduced the material recovered in the solid fraction. It should also be noted that in the case of lithium, the amount in the filtrate side was also due to the electrolyte lithium salt dissolved in the liquid.

Table 6. Anode ultrasonication delamination solvents separation efficiency results.

Solvent	Concentration (M)	Separation efficiency (%)
Deionised Water	-	100.00
Oxalic Ac.	0.05	100.00
	0.1	100.00
Citric Ac.	0.05	100.00
	0.1	100.00

In terms of separation, the three solvents showed a 100% separation efficiency, so, deionised water should be selected as solvent agent for the delamination of

anode foils to detach graphite. It was known from previous analysis that anode binder was CMC/SBR which had a high-water solubility. In this case, deionised water is selected as the suitable solvent for the anode delamination (Table 6).

Automated dismantling was studied performing manual dismantling of selected cells and proposing solutions to improve each dismantling step through robot-human cooperation (Figure 6). The net efficiency of the mechanical foil separation was analysed using mass balances to determine the amount of mass that may be lost in each pre-treatment strategy. Cell disassembly resulted in higher material recovery yields. At the completion of the disassembly procedure, up to 98.6% of the material was recovered. Some recovered fractions were suitable for direct reuse, while others facilitate the recycling stage due to the lack of other material interferences. The feasibility for automatization through robot-human cooperation was studied taking into account the different steps that need to be taken to recover all the material fractions separately. The steps were the safe discharge of the module, the module opening, the cell removal, the cell opening, the winding removal and finally the recovery of electrodes and spacer from the winding. A more detailed description of the results is summarised in deliverable D3.2.

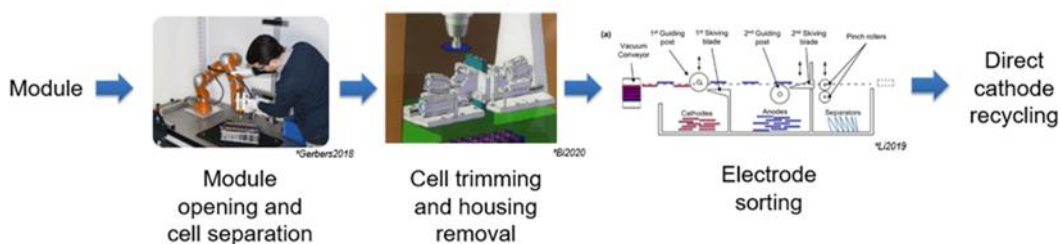


Figure 6 . Required steps for cell dismantling from the discharged module to the electrodes

4.2 Methodology to scale-up

After acquiring processing data and product results from ST3.2.1, ACCUREC is going to design the mechanical pre-treatment process at TRL 6. The initial test results from ST3.2.1 was also considered into the process design. The main results such as processing parameters for thermal pyrolysis should be ensure that the cell itself can reach more than 500°C, so that, the PVDF can be decomposed, and the cathode yield should be higher. For mechanical pre-treatment, a cutting mill will be used, and subsequent sieving should be separating material until the pore size of 1 mm. This ensures the quality of black mass and processing quantity of batteries. All these parameters will be considered for the up-scale of mechanical pre-treatment in the next reporting period of the project.

Currently an experimental facility for electrohydraulic fragmentation (EHF) of electronic scrap, type EHF-400 (ImpulsTec GmbH) is operated by FRAUNHOFER at their site in Alzenau (Figure 7). For this shock system, two reactor containers can be used with a volume of approx. 30 L or 40 L, respectively. Material volumes between 0.5 and 10 L and between 2 and 10 L

can be processed per batch in each reactor. In order to meet the goals of the scale-up T4.2, a new continuous system was designed and ordered, which is to be set up at the second location in Hanau. The implementation of the new EHF process leads to the treatment of 40-50 kg cells per hour including an automated skimming and sieving process of the EHF output to result in the separation of three desired fractions (25 kg/h of black mass, 8-10 kg/h of metals and 5 kg/h of polymers). This is equivalent to an upscale by a factor of 10.

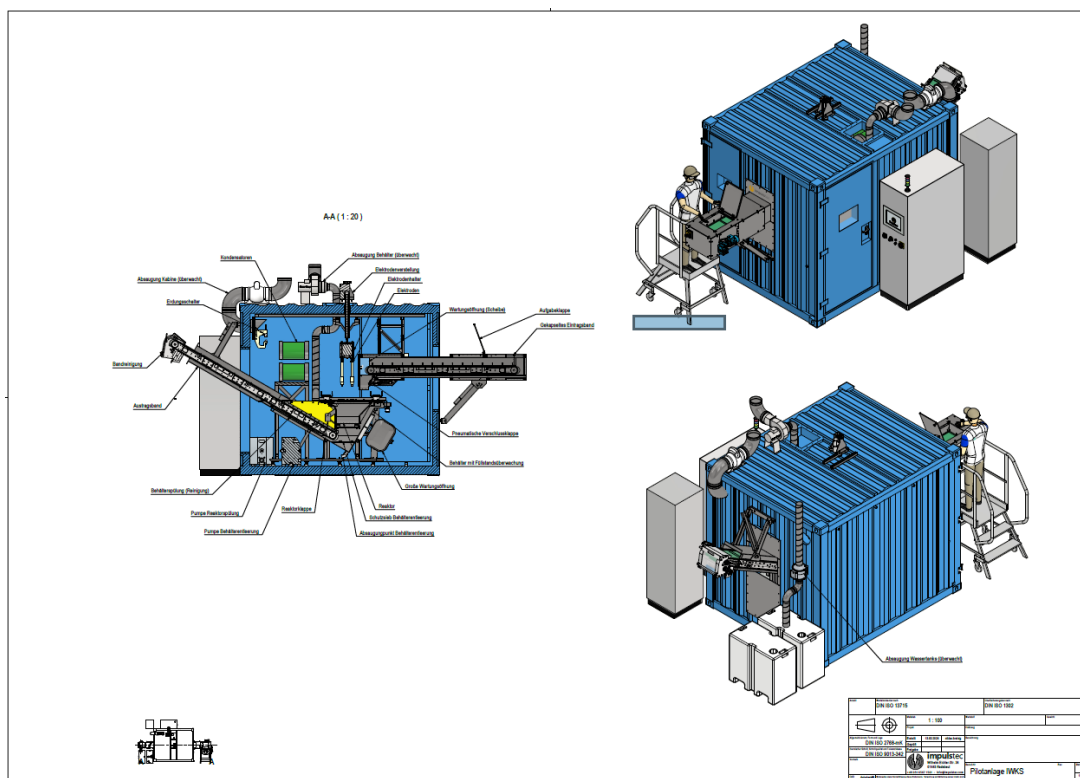


Figure 7. Final plant design of new continuous EHF (ImpulsTec GmbH) at FHG location in Hanau.

Several test series on the batch-operated system are accomplished in T3.2 and the parameters are set and optimized for the scale-up (see D3.2 Pre-treatment and sorting processes description, analysis and technical feasibility). Discussions regarding detailed planning and final implementation of the system have largely been completed. Delivery date has been postponed again to September 2024 and the setup and start-up is now scheduled for October. Further preparations for the delivery and commissioning of the system are completed.

Once the ultrasonic non-breaking delamination process has been optimized on a laboratory scale in ST3.2.3, this process will be scaled in this subtask to achieve CAM to carry out direct recycling processes. CARTIF has carried out its own design of the scaled ultrasound delamination process to have a process be able to treat minimum of 50 cathode foils per day.

5. Recycling of black mass

5.1 Results

Previously, two different approaches were assessed to investigate recycling solutions for black masses at lab scale to recover the metals of interest contained in black masses. A hydrometallurgical treatment of black mass, as well as a combined pyro-hydrometallurgical processes were analysed. Both consist of several steps that were investigated. Figure 8 and Figure 9 show the flow diagrams for the hydrometallurgical process and for the combined pyro-hydrometallurgical process carried out.

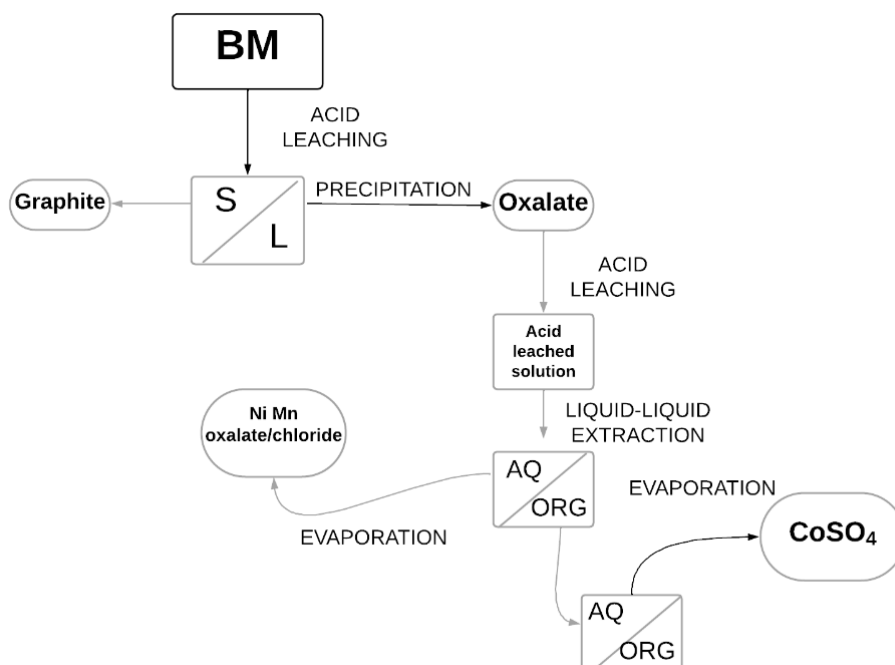


Figure 8. Flow diagram for the hydrometallurgical process

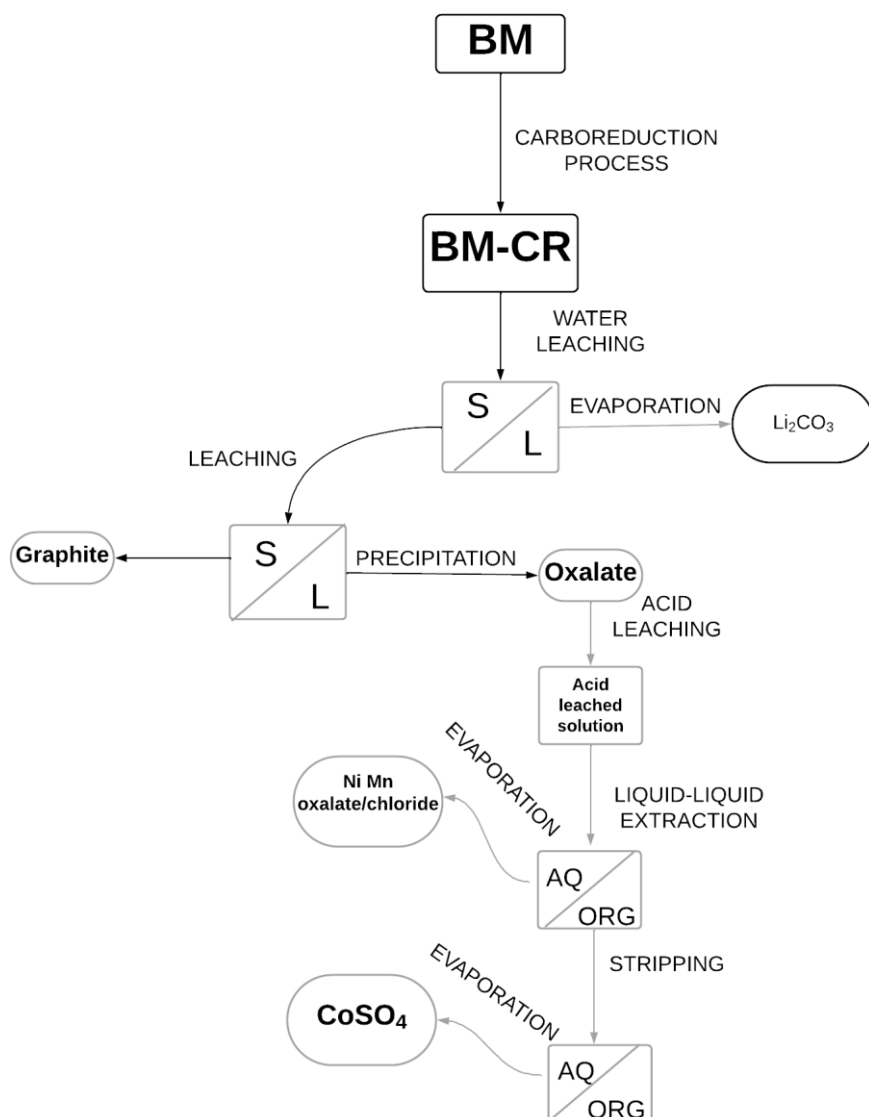


Figure 9. Flow diagram for the combined pyro-hydrometallurgical process

The chemical composition of black masses received from the different dismantling processes carried out in the project are collected in Table 7. BM01 comes from thermo-mechanical dismantling process, while BM03 comes from electrohydraulic fragmentation. The chemical composition of each black mass is the basis for the metal recovery calculation showed further on.

Table 7. Chemical composition of BMs determined by AA.

% (w/w)	BM01	BM03
Li	3.6	2.75
Ni	11.3	16.58
Co	3.3	5.15
Mn	3.9	4.20
Al	1.6	1.01
Fe	0.03	1.35
Cu	0.5	3.23
C _{total}	54.2	40.3

The precursors obtained after the recycling process are:

- PRE03: Ni, Co, Mn oxalate: obtained after the precipitation of acid leaching solution from black mass (hydrometallurgy process) or the precipitation of acid leaching solution of the residue obtained after carboreduction and water leaching (pyro-hydrometallurgical process).
- PRE05: Ni, Mn oxalate/chloride: obtained from aqueous phase after liquid-liquid separation of PRE03 acid leaching (both processes).
- PRE04: CoSO₄: obtained by evaporation of aqueous stripping phase of organic phase after liquid-liquid separation of PRE03 acid leaching.
- PRE01: Li₂CO₃: obtained by evaporation of the water leaching solution of carboreduction solid residue.
- PRE02_2: graphite residue: insoluble residue obtained after the acid leaching of water leaching carboreduction residue.

After both processes, the precursor obtained were characterized by AA and XRD. These precursors will be the basis for the synthesis of novel active materials.

XRD patterns of PRE03 obtained from hydrometallurgical and pyro-hydrometallurgical processes are shown in Figure 10. Both correspond to a metal oxalate mainly nickel, cobalt and manganese oxalate according to XRD. AAS results show that main components of the precursors are Ni, Mn and Co, with small quantities of impurities of Li, Cu and Fe (Table 8).

PRE03 was leached using HCl 10 M to separate Co by liquid-liquid extraction using a deep-eutectic solvent (DES) selective to Co. Once the organic phase is loaded with Co, the stripping of Co into an aqueous phase is performed using H₂SO₄ 0.5M, leading to PRE04 from BM01 and BM03, respectively for both

processes. PRE04 was characterized by XRD (Figure 11). As it can be observed, $\text{CoSO}_4 \cdot \text{H}_2\text{O}$ is the only mineralogical phase detected. Despite this, after the digestion of solids obtained some amounts of other impurities were also detected by AAS, as can be appreciated in Table 9.

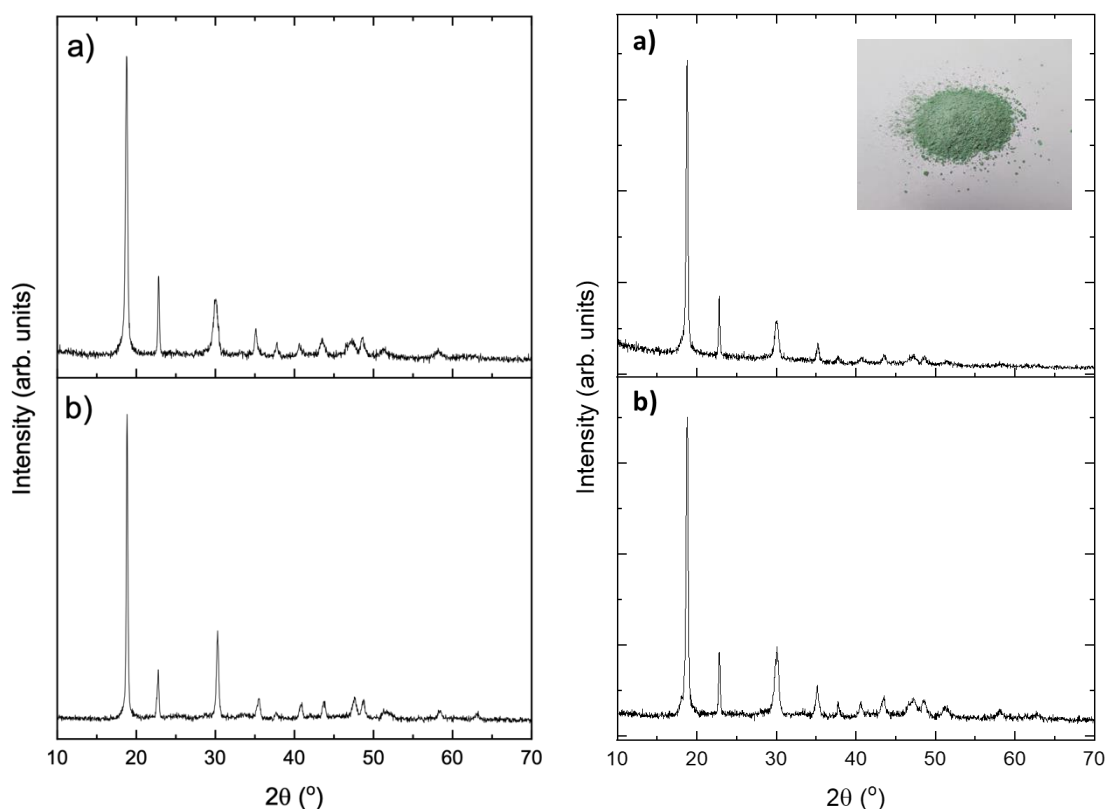


Figure 10. left: hydrometallurgical process; right: pyro-hydrometallurgical process: Ni, Mn, Co oxalates (PRE03) from (a) BM01 and (b) BM03.

Table 8. Chemical composition of PRE03.

	Hydrometallurgical process		Pyro-hydrometallurgical process	
% (w/w)	PRE03 from BM01	PRE03 from BM03	PRE03_2 from BM01	PRE03_2 from BM03
Li	0.24	0.11	0.11	0.08
Ni	16.05	14.47	17.91	17.44
Co	5.90	5.57	5.71	5.48
Mn	6.83	4.43	4.59	6.11
Fe	<0.01	<0.01	<0.01	<0.01
Cu	<0.01	4.78	0.03	0.01

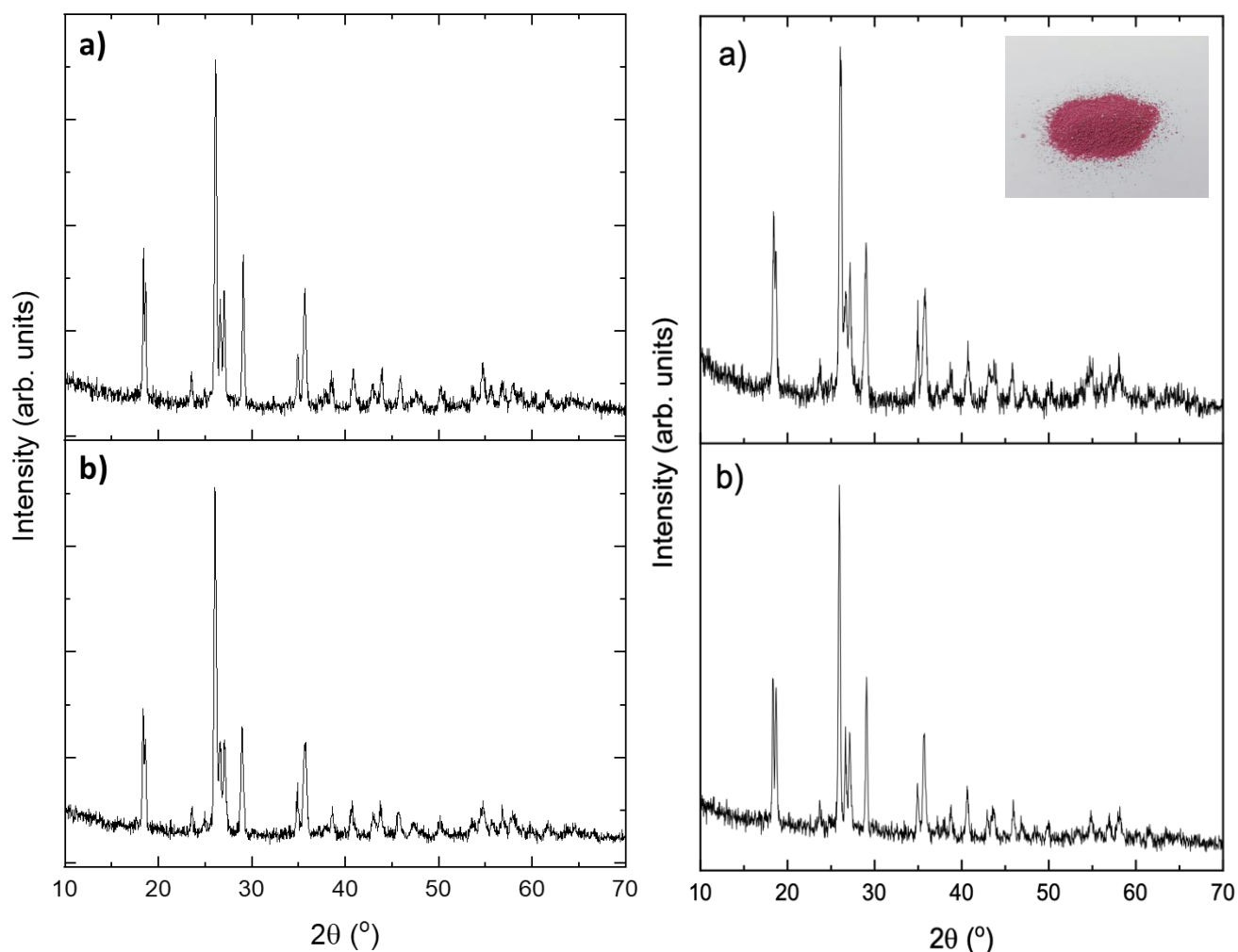


Figure 11. left: hydrometallurgical process; right: pyro-hydrometallurgical process: XRD patterns for CoSO_4 from (a) BM01 and (b) BM03.

Table 9. Chemical composition of CoSO_4 obtained from BM01 and BM03.

% (w/w)	PRE04 from BM01	PRE04 from BM03	PRE04_2 from BM01	PRE04_2 from BM03
Li	0.01	0.01	<0.01	0.01
Ni	0.75	0.79	1.46	0.79
Co	13.41	17.68	20.38	17.68
Mn	5.06	5.99	9.58	5.98
Cu	-	7.81	0.99	7.81

Then, the aqueous phases after the separation of the Co-loaded organic phases were evaporated until the final Ni/Mn-precursors solids were reached (PRE05).

The chemical compositions of the solids were calculated from AA measurements after the digestion of the powders (see

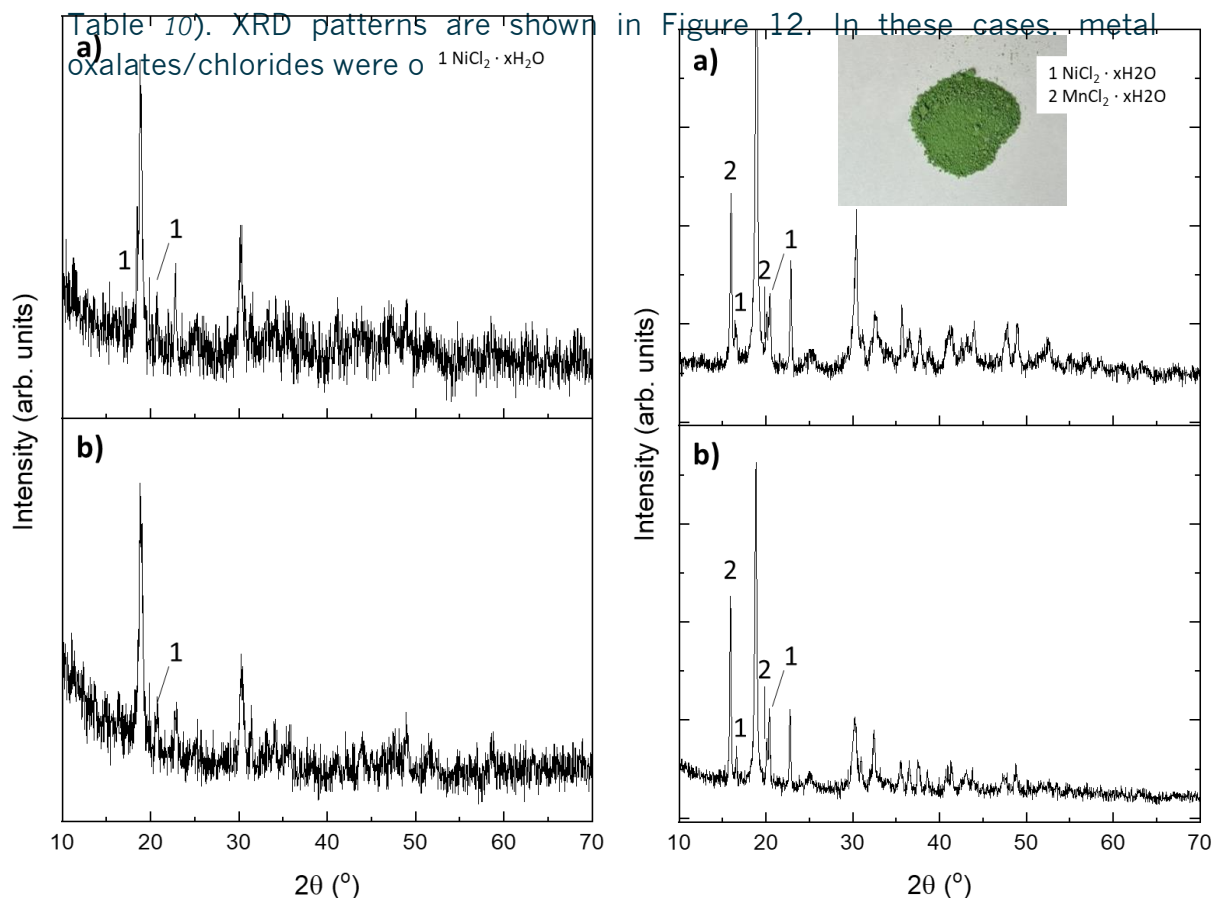


Figure 12. XRD patterns for PRE05 from (a) BM01, and (b) BM03.

Table 10. Chemical composition of oxalate/chloride obtained after Co extraction.

% (w/w)	PRE05 from BM01	PRE05 from BM03	PRE05_2 from BM01	PRE05_2 from BM03
Li	0.36	0.33	0.14	0.10
Ni	20.28	22.15	25.63	22.22
Co	0.69	0.58	0.65	0.56
Mn	6.54	4.49	4.55	5.37
Cu	-	1.16	0.01	0.006

In the case of PRE01 was only obtained for the combined process. After the carboreduction reactions tests, the reduced black mass was leached using water and the solution was evaporated, leading to PRE01. XRD of the precursors obtained for both black masses are collected in Figure 13. PRE01 is mainly composed by Li_2CO_3 , with impurities of LiF (

Table 11). Mineralogical composition calculated from the chemical composition of PRE01 is shown in Table 12.

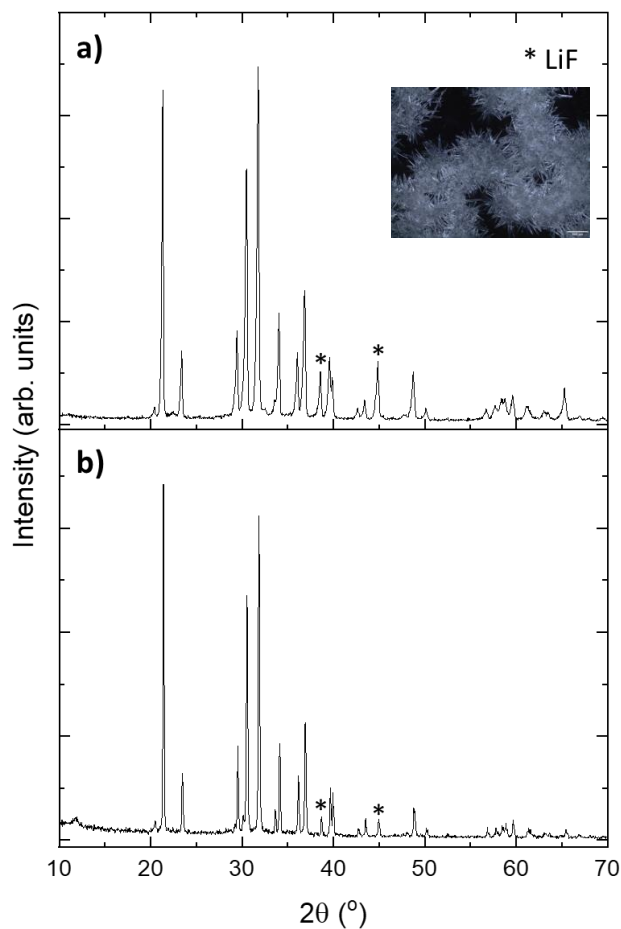


Figure 13. XRD for PRE01 precursors, a) BM01, b) BM03

Table 11. Chemical composition of PRE01 by AA.

% (w/w)	PRE01 from BM01	PRE01 from BM03
Li	17.29	17.44
F	0.85	0.61

P	0.09	0.06
---	------	------

Table 12. Mineralogical composition calculated for PRE01 precursors by AA.

	PRE01 from BM01	PRE01 from BM03
Li ₂ CO ₃	90.59%	91.98%
LiF	1.15%	0.83%
Li ₃ PO ₄	0.31%	0.23%

PRE02_2 is the solid residue obtained after the carboreduction process + water leaching + acid leaching. This residue is mainly composed by graphite, with some metal impurities that are shown in Table 13.

Table 13. Chemical composition of PRE02_2 by AA.

% (w/w)	PRE02_2 from BM01	PRE02_2 from BM03
Li	0.08	0.08
Ni	2.54	3.19
Co	0.92	0.86
Mn	0.05	0.05
Fe	<0.01	<0.01
Cu	2.25	2.15

Table 14 summarizes the recovery of each metal using both processes (i.e. hydrometallurgical and combined pyro- and hydrometallurgical). The obtained percentages were calculated from both black masses with different pre-treated steps (i.e. BM01, thermo-mechanical pre-treatment process; and BM03, electrohydraulic fragmentation process). The recovery rate of each metal was calculated following equation 1:

$$\% Me = \frac{[Me]_{PRE}}{[Me]_{BM}} \times 100 \quad \text{Equation 1}$$

where [Me]_{PRE} is the concentration of the metal in the precursor studied, and [Me]_{BM} is the initial concentration of the metal in the black mass.

Table 14. Recovery of each metal (in %) from BM01 and BM03 black masses, by both processes assessed.

Element	Precursor type	Hydrometallurgical process		Combined pyro-hydrometallurgical process	
		BM01	BM03	BM01	BM03
Li	Li ₂ CO ₃	-	-	69.1	74.8
Ni	Ni, Mn, Co oxalate	62.7	43.3	73.0	49.3
Co		78.3	52.3	59.1	68.1
Mn		66.8	53.6	67.9	49.9
Ni	Ni, Mn oxalate/chloride	69.1	39.2	75.3	18.9
Co		65.4	31.4	39.2	18.1
Mn		6.8	3.3	5.5	1.5
Co	Cobalt sulphate	34.9	41.0	50.9	31.9

In general, the recovery percentages for BM01 were higher than those obtained for BM03. Furthermore, in general terms the recovery of each metal using the combined pyro-hydrometallurgical process was higher than by the hydrometallurgical process.

It should be noted that by using the hydrometallurgical process the obtained precursors mainly contain Ni, Mn, and Co while Li (which is a critical and strategic metal) remains in the solution. However, in the case of combined pyro- and hydrometallurgical processes, Li can be recovered as Li₂CO₃.

For these reasons, the combined pyro-hydrometallurgical process is chosen to develop the scale-up technologies for the Li-ion batteries recycling.

5.2 Methodology to scale-up

After the optimization of the experimental conditions at the lab scale, metals recovery was evaluated by scale-up technologies. It should be noted that it may be necessary to optimize again the experimental conditions. The obtained results will be compared with those previously obtained at laboratory scale.

Different approaches will be assessed to improve the recovery of metals from each black mass:

- Recovery of Li: the black mass which was subjected to thermo-mechanical pre-treatment process (i.e. BM01) will previously be water leached for the recovery of Li.
- Recovery of Ni, Mn, Co as oxalate: a needed step to obtain the corresponding metals oxalates, is malic acid leaching. This leaching step will be optimized, and reaction time, solid/liquid ratio, as well as number of steps will be analyzed. It should be noted that the precipitation step was successfully developed at lab scale with quantitative precipitation of all metals.
- Recovery of Co: conditioning of the extraction reagent at the liquid-liquid extraction step will be investigated in order to improve Co separation.
- Recovery of Ni, Mn as oxalate/chloride: the separation of Ni and Mn will be assessed. For of all, different experiment will be evaluated at lab-scale, as previously investigated for each metal. In the case of satisfactory results, up-scaling technology will be evaluated.
- Recovery of graphite: graphite residue from carboreduction insoluble residue acid leaching. Purification of PRE02_2 by strong mineral acid leaching to remove metal impurities will be evaluate in case improvement of PRE02_2 if needed.

To carry out the scale-up experiments, the following steps and equipment will be employed:

STEPS	EQUIPMENT
-------	-----------

CARBOTHERMIC REDUCTION REACTION

Vertical tubular electrical furnace with 5kg of capacity equipped with a N₂ carrier input



WATER LEACHING

Jacketed glass reactor vessel with 10L of capacity,



EVAPORATIVE CRYSTALLIZATION TO OBTAIN PRE01

Rotavapor
with 10l of
capacity



ACID LEACHING

Jacketed
glass reactor
vessel with
10L of
capacity,



SELECTIVE PRECIPITATION (PRE03)



Jacketed
glass
reactor
vessel with
10L of
capacity,



ACID LEACHING

Jacketed
glass reactor
vessel with
10L of
capacity,



<p>EXTRACTION AND STRIPPING</p>	<p>Liquid-liquid extraction funnels with 1L of capacity</p>	
<p>EVAPORATIVE CRYSTALLIZATION TO OBTAIN PRE04 & PRE05</p>	<p>Rotavapor with 10L of capacity</p>	

6. Cathode direct recycling processes

6.1 Results

Cathode direct recycling processes have been developed until TRL 4 for following 3 technologies: 3a - NADES leaching of cathode paste, 3b – Re-Lithiation of cathode paste and 3c – Electrochemical re-lithiation of cathode foil and their achieved results are described in Deliverable D3.3 “Development, testing and validation of recycling solutions for cathode and black mass at lab-scale”.

The direct recycling throughout NADES leaching of cathode paste experimental procedure at TRL 4 has been developed from TRL 2 as is explained in D3.3 showing recovery rates of 53% for lithium, 99.7% for nickel, 99.9% for manganese, and 99.7% for cobalt.

Re-Lithiation of cathode paste and foil have been both successfully achieved restoring the loss of the Li ions in the cathode, recovering its original composition and crystalline structure to NMC 622. Aiming on that, the following section explain the procedure that will be followed for the implementation of the scaling-up of both technologies. In the following Table 15, it is shown the percentage of Lithium re-introduced in the electrode composition throughout the re-lithiation technologies.

Table 15. Most promising results of Lithium restoration achieved with Re-lithiation technologies

Re-lithiation route	Content of Lithium	
	Original (wt%)	Restored (wt%)
Hydrothermal	6.21	7.82
Electrochemical	6.87	7.13

Both technologies give the opportunity to restore the composition of the cathode. Hydrothermal route from the Cathode Active Material (CAM) delaminated before by ultrasonic delamination technology (2d) and Electrochemical route from Cathode foil after the manual dismantling of KONA cells.

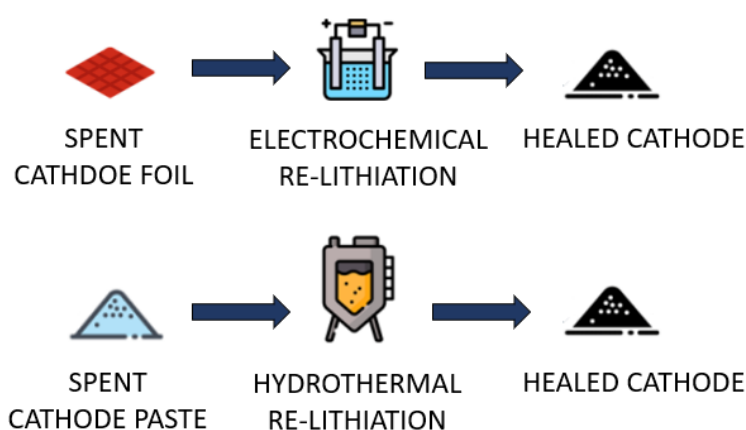


Figure 14. Re-lithiation technologies to restore cathode active material.

6.2 Methodology to scale-up

The direct recycling throughout NADES leaching of cathode paste experimental procedure at TRL 4 has been developed, however due to the uncertainty of the use of this technology as direct recycling route it was considered at the proposal stage preparation as the limit TRL 4, so its scale-up is not going to be implemented to TRL 5-6 within WP4 and the research in this technology finished in month 24 of the project. Although the methodology followed in the WP3 for scaling this technology from TRL 2 to 4 is detailed in D3.3.

On the other hand, the re-lithiation routes studied within WP3 will be scale-up for its development and further research aiming to achieve a large solutions will be developed.

For Hydrothermal route, the results of the study of variables and experimental procedures followed at lab scale will be optimised and developed in a larger reactor of 2L where the test previously carried out will be repeated enabling to validate the hydrothermal process and produce enough healed CAM for its further re-use in the manufacturing of new cells within WP4.

The experimental tests for Hydrothermal re-lithiation will be carried out in a PARR reactor 4520 as shown in the Figure 15.



Figure 15. 2000mL Parr pressurised reactor for Hydrothermal re-lithiation.

Regarding the Electrochemical re-lithiation, as described in the DoA, the first stage of this research was just achieved with the validation of the technology at from TRL 2 to 4. For the upcoming months, the target to realise the TRL 5 will be to achieve a complete re-lithiation of an entire cathode electrode optimising the variables studied in the WP3.

The experimental tests for Electrochemical re-lithiation will be carried out in a larger electrochemical cell than the one used on a lab scale.

7. Recycling of plastics

7.1 Results

Task 3.5 Recycling of plastics at lab-scale has focused on the recovery of plastic components and parts from EoL batteries in EVs after performing dismantling operations. AIMPLAS has collected different plastic components sent by several partners.

The first stage in the pre-treatment of plastic components consisted of the sorting and classification of plastic parts according to shape, size and functionality. Figure 16 shows the different plastic parts extracted from battery pack HYUNDAI KONA EV.




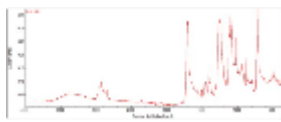

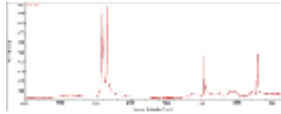

Figure 16. Plastic parts extracted from battery pack dismantling.

The second stage has included the identification of polymer types by means of visual inspection and optical analysis of plastic parts samples applying Near Infra-Red (NIR) spectroscopy using of handheld NIR analyser or Fourier Transform Infrared spectroscopy (FTIR) using laboratory analyser.

Table 16 summarizes results of material identification analysis for the plastic parts extracted from EV battery pack.

Table 16. Plastic components identification results.

	Plastic part & function (weight)	Manufacture method	Polymer type	Identification technique
	Protective and insulation panels (250 g)	Compression moulding	Polypropylene PP	Visual, FTIR 
	Liquid cooling system tubes (25 g)	Extrusion	Polyamide PA 11	Visual, FTIR 
	Tube fittings (6 g)	Injection moulding	Polyamide PA 66	Visual, FTIR 
	Module cell pouch frames (92 g)	Injection moulding	Polyphenylene Ether PPE	Visual, FTIR 
	Connector protective covers (50 g)	Injection moulding	Polypropylene PP	Visual, NIR 

	Connector protective plates (10 g)	Injection moulding	Polyacrylonitrile-Butadiene-Styrene ABS	Visual, FTIR 
	Air cooling system duct (125 g)	Injection moulding	Polyethylene HDPE	Visual, FTIR 
	Sealing rubber band (550 g)	Compression moulding	Synthetic rubber EPDM	Visual

The definition of the most feasible case studies for plastic components recycling has considered component functionality and material source availability and suitability for upscaling operations in further *WP4 Task 4.5 Scale-up for plastic materials recycling*.

- Case study #1 : Cell pouch frames from battery modules
- Case study #2 : Tubes from cooling system
- Case study #3 : Protective and insulating panels

For each case study the benchmarking polymer types and grades have been set according to product performance requirements. Depending on each plastic component, several pre-treatment operations have been performed with the aim of obtaining material samples and test specimens to perform material properties characterization at laboratory level. Deliverable *D3.4 Report on plastic materials recovered and properties characterization* details thoroughly the activities and testing performed for each case study. A summary is provided in the following sections.

7.1.1 Case study #1 Cell pouch frames

EV battery packs include several modules consisting of cell pouches connected and held by frames stacked. Frames are manufactured using thermoplastic polymer type polyphenylene ether (PPE) by means of injection moulding. Figure 17 shows frame after removing cell pouch.



Figure 17. Cell pouch frames from battery modules.

Cell frames incorporate metal inserts for connectors that are overmoulded in the manufacturing process. These metal inserts need to be removed in order to recycle the thermoplastic part. The first stage in the pre-treatment consists of part crushing in order to reduce the part size down to particles size 20-60 mm. The second stage consists of metal separation by means of magnet rods that capture the ferrous inserts and Eddy currents for non-ferrous metal separation. As a result of this stage, the metal fraction is removed from the plastic parts stream (metal fraction in a single frame represent approximately 62%(w/w)). So that the next stage consists of the grinding of the plastic fraction using a shredder mill to obtain grinded plastic granulates with smaller particle size 4-8 mm. In order to perform plastic material characterization standard test specimens have been obtained from rPPE plastic granulates by means of injection moulding. Figure 18 depicted flow diagram for recycling case study #1.

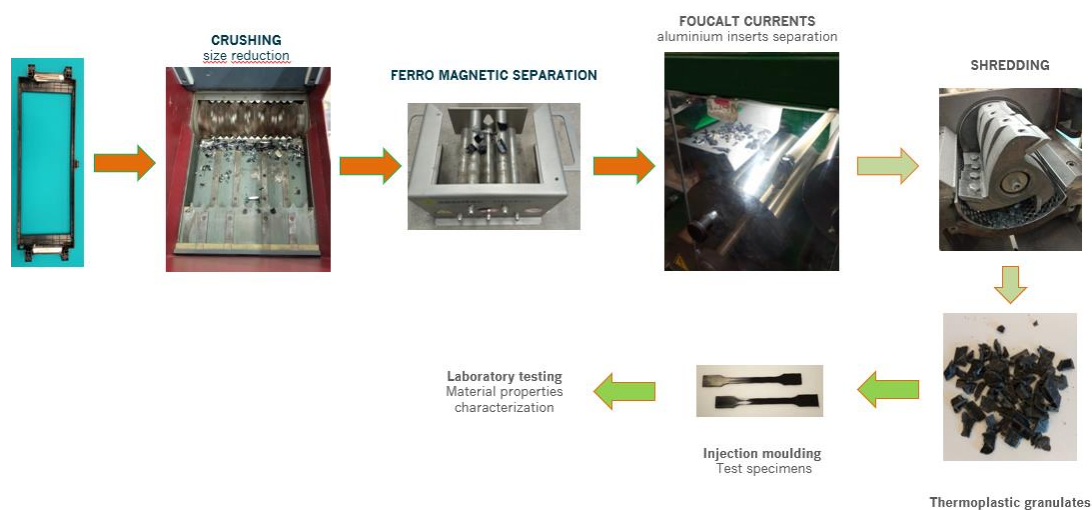


Figure 18. Flow diagram for lab recycling case study #1 Cell pouch frames.

Table 17 summarises results from laboratory tests comparing the recycled material rPPE recovered from module frames to the benchmark material.

Table 17. rPPE material properties characterization.

Property	Test method	Unit	Bechmark polymer NORYL™ RESIN NHP6012 10% GF	Recycled polymer rPPE from EV battery module frames
Tensile stress at break	UNE-EN ISO 27	MPa	82	78.1
Tensile strain at break	UNE-EN ISO 27	%	2.5	3.1
Flexural modulus	UNE-EN ISO 178	MPa	4000	4050
Flexural strength	UNE-EN ISO 178	MPa	132	118
Charpy impact resistance Notch @ 23°C	UNE-EN ISO 179/1eA	kJ/m ²	6	9.64
Charpy impact resistance Unnotch @ 23°C	UNE-EN ISO 179/1eU	kJ/m ²	25	34.58
Heat Deflection Temperature 1.8 MPa	UNE-EN ISO 75	°C	125	122

Heat Deflection Temperature 0.45 MPa	UNE-EN ISO 75	°C	132	128
Rockwell M hardness	UNE-EN ISO 2039	..	90	167

Results from material tests performed on recycled polymer rPPE from EV battery module frames show that there is a decrease in mechanical properties related to tensile and flexural strength when compared to benchmark polymer. There is a 5% decrease in tensile stress and a 10% decrease in flexural strength. Also, there is approximately 3% decrease in heat deflection temperature (HDT). Nevertheless, recycled material shows higher impact resistance (for both notched and unnotched tests) and hardness. These overall results suggest that service conditions have led to some losses in the material toughness and thermal resistance.

7.1.2 Case study #2 Pipes and fittings cooling system

EV battery packs are equipped with an internal liquid cooling system to manage temperature and prevent battery damage. This is crucial because batteries generate heat during charging or discharging and this affects performance, safety and battery degradation. The cooling system consists of different pipes and tubes that conduct the cooling liquid throughout the system.

Pipes are manufactured using thermoplastic polymer type polyamide (PA11) by means of extrusion. Figure 19 show pipe featuring Ø 16 mm.



Figure 19. Pipes extracted from battery pack cooling system.

Pipes and tubes are connected using fittings as depicted in Figure 20. Fittings are manufactured using thermoplastic polymer type polyamide (PA66) by means of injection moulding.



Figure 20. Fittings extracted from battery pack cooling system.

The first stage in the pre-treatment consists of disassembling of pipes manually removing fittings from tubes. The second stage consists of the grinding of the plastic components using a shredder mill to obtain grinded plastic granulates with smaller particle size 4-8 mm. In order to perform plastic material characterization standard test specimens have been obtained from rPA plastic granulates by means of injection moulding. Figure 21 depicted flow diagram for recycling case study #2.

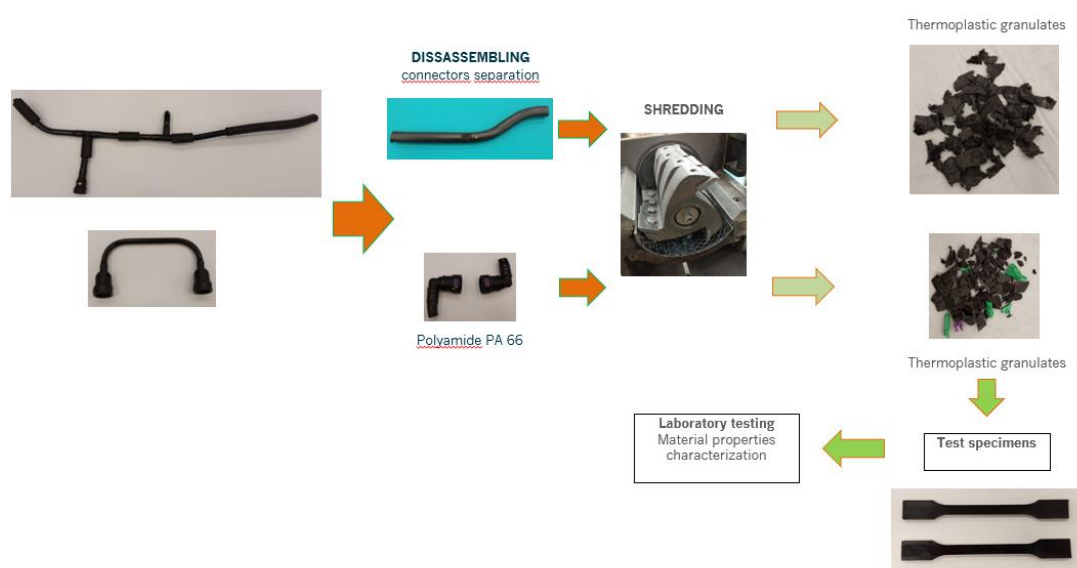


Figure 21. Flow diagram for lab recycling case study #2 Cooling system pipes and fittings.

Regrettably the amount of rPA11 granulates recovered from pipes were not enough to run the injection moulding process not allowing the manufacture of sufficient test specimens for the whole set of tests. Additional samples of PA11 tubes are being collected to perform further recycling. Instead, in the case of rPA66 granulates, enough material was available for the manufacture of test specimens by means of injection moulding. Table 18 summarises results from laboratory tests comparing the recycled material rPA66 recovered from fittings to the benchmark material.

Table 18. rPA66 material properties characterization.

Property	Test method	Unit	Benchmark polymer LEONA™ 1402S	Recycled polymer rPA66 from fittings
Tensile stress at break	UNE-EN ISO 27	MPa	82	77.2
Tensile strain at break	UNE-EN ISO 27	%	4.0	2.2
Flexural modulus	UNE-EN ISO 178	MPa	2700	5050
Flexural strength	UNE-EN ISO 178	MPa	113	141
Charpy impact resistance Notch @ 23°C	UNE-EN ISO 179/1eA	kJ/m ²	6.0	6.3
Charpy impact resistance Unnotch @ 23°C	UNE-EN ISO 179/1eU	kJ/m ²	No break	32.44
Heat Deflection Temperature 1.8 MPa	UNE-EN ISO 75	°C	70	233
Heat Deflection Temperature 0.45 MPa	UNE-EN ISO 75	°C	190	243
Rockwell M hardness	UNE-EN ISO 2039	..	80	177

Results from material tests performed on recycled polymer rPA66 show that there is a decrease in mechanical properties related to tensile strength and strain when compared to benchmark polymer (decrease is approximately 6% and 45% respectively). The mechanical behaviour related to other properties

(such as flexural modulus, flexural strength) that are noticeably higher than the benchmark polymer suggest that service conditions have led to significant losses in the material toughness as well as increased rigidity.

7.1.3 Case study #3 Protective and insulating panels

EV battery pack include different large dimension panels that helps to protect battery modules and other components from vibrations and impacts, while also providing electrical and thermal insulation, minimizing the risk of thermal runaway. Panels are manufactured using thermoplastic polymer type expanded polypropylene (EPP) by means of extrusion or moulding foaming. The foaming process allows to manufacture very lightweight parts (material density range from 20 kg/m³ to 200 kg/m³ depending on the specific formulation and manufacturing process) and the foam cell structure features numerous air pockets contributing to thermal insulation. Figure 22 shows different PP foamed panels extracted after EV battery pack dismantling.

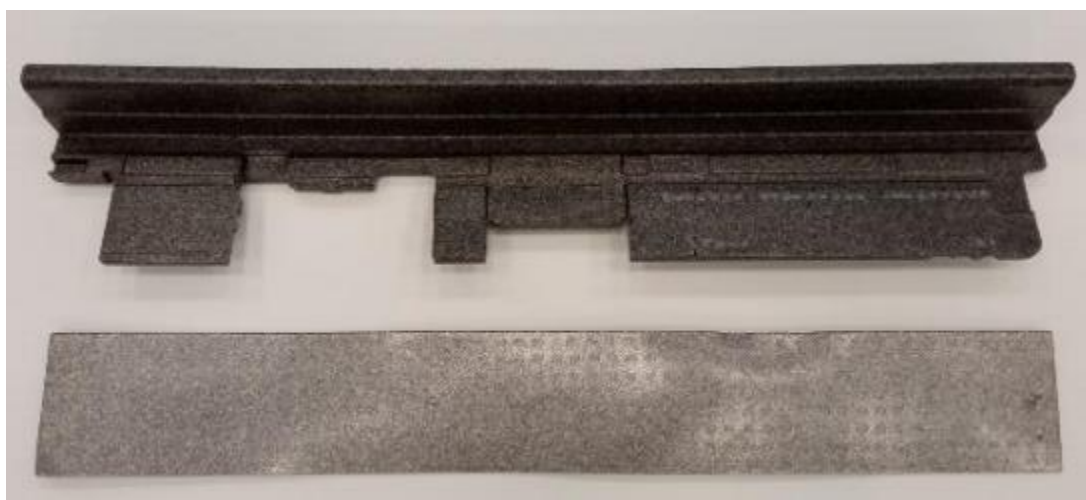


Figure 22. EPP foamed extracted from EV battery pack.

The first stage in the pre-treatment consists of the grinding of the EPP panels using a shredder mill to obtain grinded plastic granulates with smaller particle size (4-6 mm). The second stage in the pre-treatment consists of the agglomeration of PP granulates into pellets offering higher bulk density. For that purpose, the equipment used is an agglomeration mill featuring a rolling presser. As an outcome the PP material granulates are agglomerated in the form of densified pellets size 6-8 mm. Although PP densified pellets obtained after agglomeration exhibit higher bulk density (in the range 0.4-0.5 kg/m³), still it is not enough to assure continuous feeding in reprocessing equipment, and also the pellets morphology tends to disaggregate into powders. So that the next pre-treatment stage has consisted of the melt extrusion of PP densified

pellets by means of twin screw co-rotating extruder in order to obtain uniform rPP pellets particle size 4-6 mm. Figure 23 depicted flow diagram for recycling case study #3.

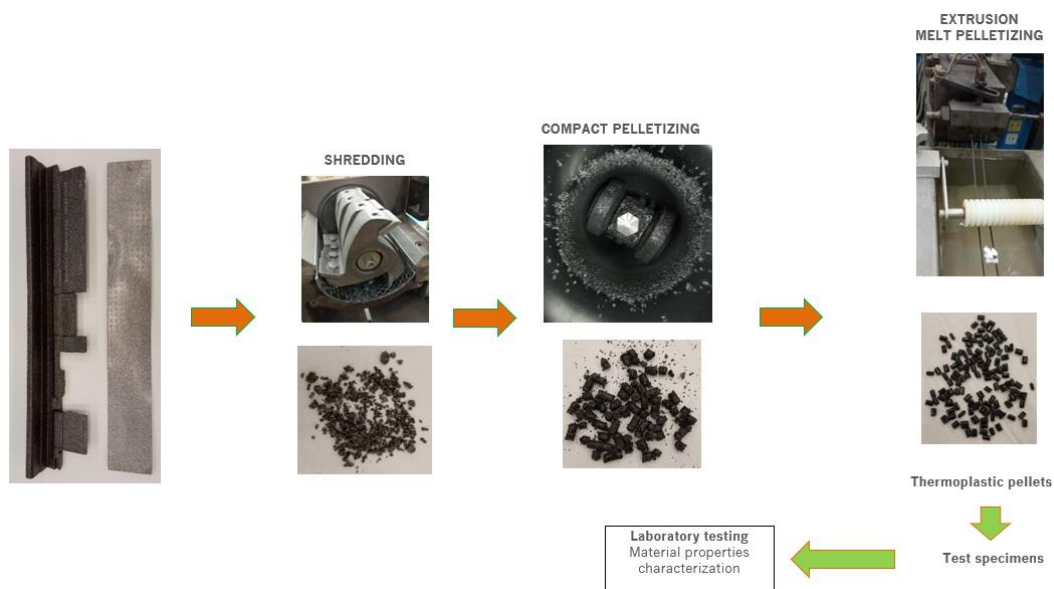


Figure 23. Flow diagram for lab recycling case study #3 insulation and protective panels.

In the case of EPP panels, properties characterization has consisted in the determination of foamed panels density and analysis of cell structure. Density result is included in Table 19. Figure 24 shows microscope image analysis of material cell structure.

Table 19. EPP panels properties characterization.

Property	Test method	Unit	EPP panels
Density	UNE-EN ISO 845	Kg/m ³	66

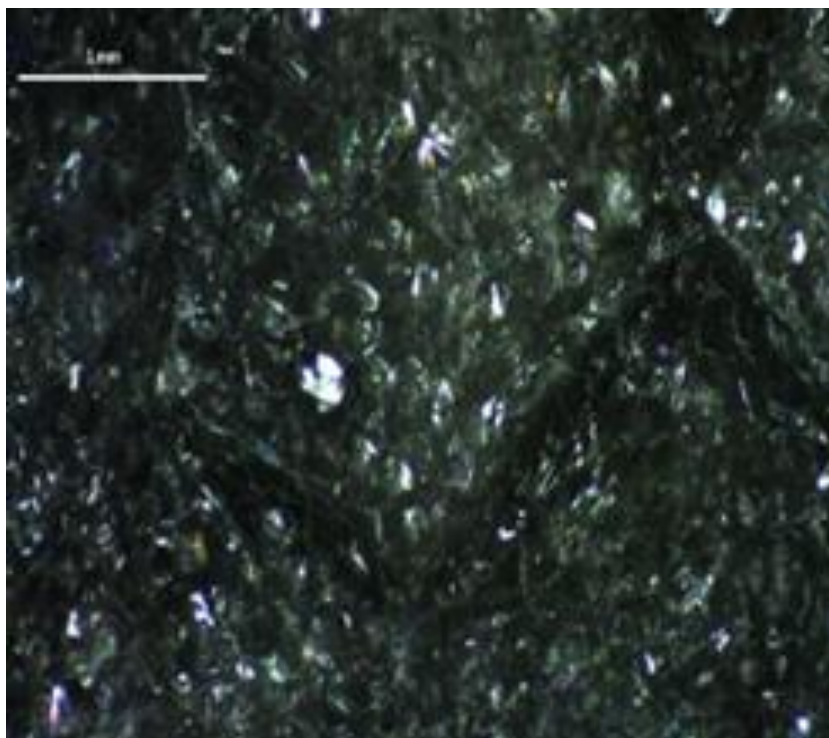


Figure 24. Microscope image analysis of material cell structure.

In addition, the recycled rPP thermoplastic granulates have been tested for melt flow index analysis. Results are included in Table 20.

Table 20. rPP material properties characterization.

Property	Test method	Unit	Bechmark polymer Daploy™ WB140HMS	Recycled polymer PP from panels
Melt flow rate	UNE-EN ISO 1133-1 (230°C/2.16 kg)	g/10 min	2.1	16.1

Outcomes from material test performed on recycled polymer rPP show higher melt flow rate suggesting that resin have a molecular structure that exhibit high flowability and lower melt strength, so that hampering foaming process stability.

7.2 Methodology to scale-up

The outcomes obtained from each case study will set the basis for reprocessing and upcycling of the recovered plastic materials in further *WP4 Task 4.5 Scale-up for plastic materials recycling*, with the aim of obtaining thermoplastic

compounds formulated for their reuse in battery plastic parts or other high value applications.

Next steps include the collection of plastic parts for each case study in order to gather enough materials (in the range 5-10 kg) for running operations at pilot plant scale. The methodology proposed for each case study is detailed in the following sections.

7.2.1 Case study #1 Cell pouch frames

Pre-treatment operations consisting of crushing, metals separation and shredding will transform plastic frames into rPPE granulates to be reused as a secondary raw material in the production of thermoplastic compounds incorporating recycled content.

As service conditions have led to some losses in the material toughness and thermal resistance, upcycling methodology is aimed to improve the performance of the thermoplastic compound by means of blending rPPE with virgin PPE pellets and reinforcing glass fibres. Additionally, specialty additives (such as compatibilizers, aid processors, etc.) will be incorporated in the formulation. Expected compound blends will incorporate 30%, 50% and 70% recycled content, featuring 10% glass fibre reinforcement.

Compounding operations will take place in AIMPLAS pilot plant using twin screw extruder (as depicted in Figure 25). This equipment allows to set up a modular extrusion line for thermoplastic reprocessing featuring modular extruder, feeding systems, degassing pumps, conveyor belts and pelletizing unit. Preliminary trials will be performed in order to optimize processing parameters: screw design, extruder temperature profile, output rate, etc.



Figure 25. Extrusion compounding line in AIMPLAS pilot plant.

As an outcome of these activities, thermoplastic pellets of rPPE compounds will be obtained in order to manufacture injection moulding test specimens for testing tensile and thermal resistance properties.

7.2.2 Case study #2 Cooling system tubes

Pre-treatment operations consisting of disassembling and shredding will transform plastic tubes into rPA granulates to be reused as a secondary raw material in the production of extruded tubes incorporating recycled content.

During service conditions tubes are prone to absorb cooling liquids (mainly ethylene-glycol) that swallow polymer matrix extracting plasticizer additives leading to material degradation and mechanical properties losses. Upcycling methodology will consider two stages.

In a first stage decontamination of rPA11 granulates will be performed using innovative extrusion technology featuring injection of CO₂ in supercritical conditions as stripping agent to remove chemical substances and volatile compounds. Decontamination operations will take place in AIMPLAS pilot plant using tandem extrusion system (as depicted in Figure 26). This equipment allows to set up a modular extrusion line for thermoplastic decontamination featuring single screw extruders, melt filters, CO₂ metering system, degassing pumps, cooling bath and pelletizing unit. Preliminary trials will be performed in order to optimize processing parameters: extruder temperature profile, CO₂ flow, output rate, etc.

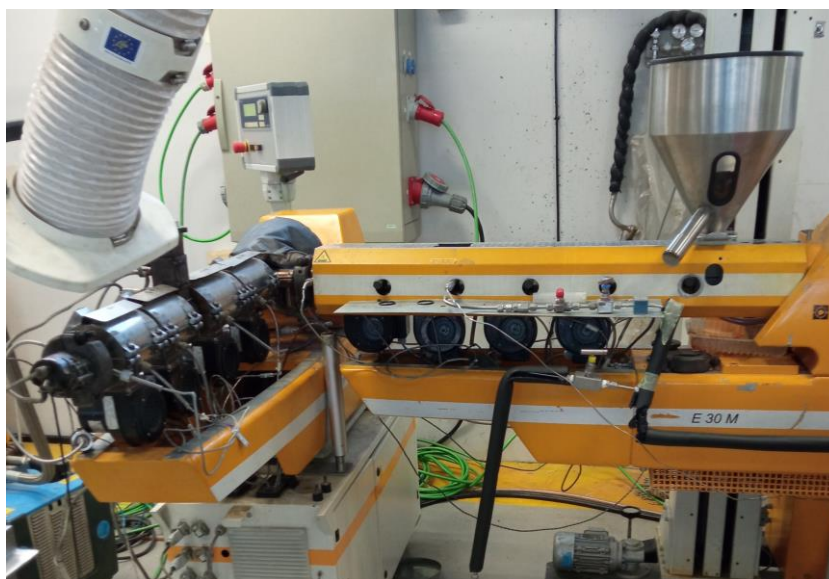


Figure 26. Tandem extrusion line in AIMPLAS pilot plant.

In a second stage, the cleaned rPA11 pellets obtained will be blended with virgin PA11 pellets and specialty additives (such as plasticizers) using a modular twin screw extruder. Expected compound blends will incorporate 20%, 40% and 60% recycled content.

As an outcome of these activities, thermoplastic pellets of rPA11 compounds will be obtained as input material to manufacture extruded tubes featuring Ø 16 mm. Extrusion operations will take place in AIMPLAS pilot plant using pipe extrusion line (as depicted in Figure 27). Preliminary trials will be performed in order to optimize processing parameters: extruder temperature profile, output rate, draw down ratio, etc. The thermoplastic rPA11 tubes obtained will be tested in laboratory for material properties characterization.



Figure 27. Pipe extrusion line in AIMPLAS pilot plant.

7.2.3 Case study #3 Protective and insulating panels

Pre-treatment operations consisting of shredding, agglomeration and melt extrusion will transform insulating panels into rPP pellets to be reused as a secondary raw material in the production of foamed products incorporating recycled content.

Extrusion foaming operations will take place in AIMPLAS pilot plant using extrusion line (as depicted in Figure 28). This equipment features dosing system for the incorporation of gas CO₂ as a physical foaming agent into the polymer matrix. Blends of rPP pellets with virgin PP pellets will be used as input materials. Additionally, specialty additives (such as nucleating agents) will be incorporated in the formulation. Expected blends will incorporate 10%, 20% and 30% recycled content. Preliminary trials will be performed in order to optimize processing parameters: extruder temperature profile, output rate, CO₂ dosing ratio, etc.



Figure 28. Foaming extrusion line in AIMPLAS pilot plant.

As an outcome of these activities, foamed products consisting in rods or stripes will be obtained and tested in laboratory for material properties characterization.

8. Recycling of metals

8.1 Results

8.1.1 Battery case disassembling and pre-melting of the aluminium alloys recovered

In WP3.6, we have investigated the recyclability of aluminium and copper through the production of powder from a range of aluminium alloys. The objective was to create a powder with the necessary characteristics to be used as a raw material for additive manufacturing via selective laser melting. To test this possibility on WP6, a series of processes and laboratory tests were carried out, the results of which are detailed in deliverable D3.5.

The starting material used to produce the powder was obtained from a Hyundai Kona 64 kWh battery that had been removed due to a malfunction, discharged and disassembled by Accurec. Structural frames, covers, cooling plates and metal separators were manually disassembled and sent to the laboratory. Only the metal parts of the battery casing were retained. Visually similar parts were grouped and weighted.

The battery case studied consists of approximately 29.3 kg of steel (including 1.5 kg of fixings) and 45.5 kg of aluminium. This battery model consists of a steel lid and a cooled aluminium base with the cell modules mounted on aluminium frames. The aluminium components are shown in Figure 29.

The composition of the different types of components was analysed by optical spark emission and Figure 30 shows the percentage by weight of each type of alloy. The battery case is constructed from a combination of five distinct aluminium alloys. The extreme covers of the modules are made from an AlSi12 casting alloy, while the internal module separators are produced using a 5xxx alloy. Two different 3xxx alloys are used for the thin cases and the cooling circuit plate, and finally, a 6xxx alloy is employed for the modules holding frames.



Figure 29. Classification of aluminium battery case parts a) module covers, b) separators, c) and d) case, e) and f) cooling floor, g), h) and i) frames.

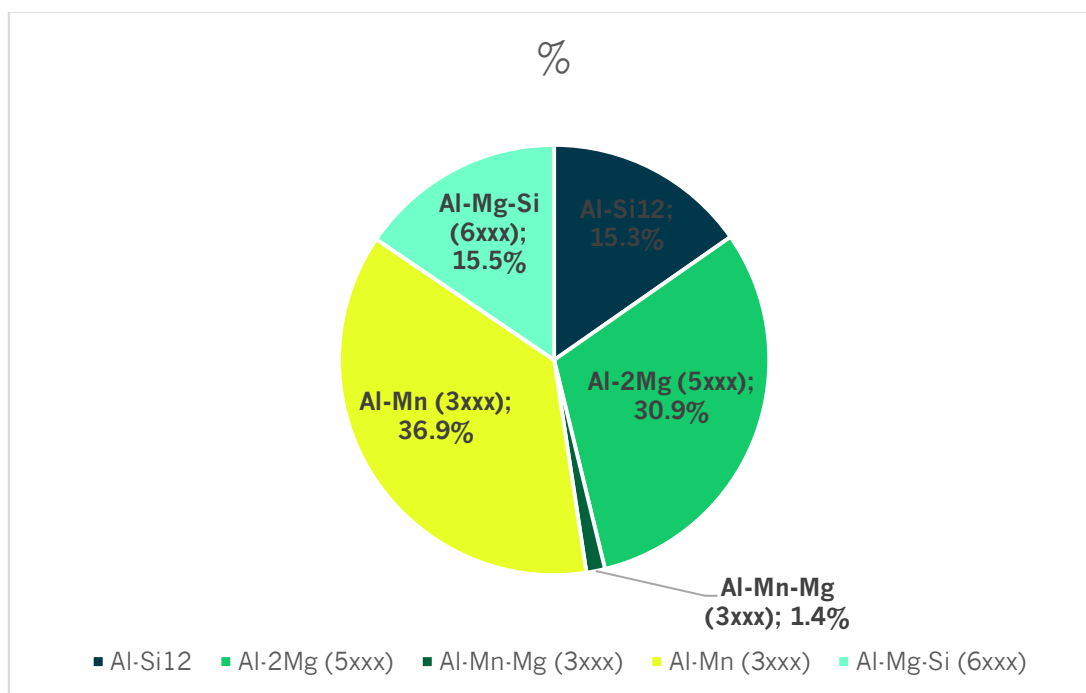


Figure 30. Battery case aluminium alloys weight breakdown

All the parts were cut with the appropriate tool, either shears or sheet metal shears, depending on the thickness of the metal sample. This was done until practical fragments were obtained, of a size that would subsequently allow the largest possible quantity of sample to be placed in a crucible for melting. In some case, as Type 2 parts, it was first necessary to remove the rubber covering one of their faces by immersing the metal sheets in acetone at room temperature until the adhesive was detached. Parts type 5 and 6 required to remove a film of polystyrene adhered to them and to clean the adhesive residue with acetone.

Components with comparable compositions were selected for casting in a single batch. The melting process was conducted in an electric furnace under aerobic conditions at a temperature of 750°C. The total weight of the ingots produced was 36,249 kg. The weight difference of -16.4% from the initial weight of all parts is due to the formation of slag and debris left in the crucible and moulds.

8.1.2 Metal powder production using Vacuum Induction Melting Inert Gas Atomization

In this project, we have selected a 7% wt Si aluminium alloy as the target for producing powder for SLM. AlSi7 is also a hypoeutectic alloy, with a silicon content of less than 11% by weight. It shares many characteristics with AlSi10Mg. Given that the alloy obtainable with the materials of this battery case

has only 2% silicon, it was decided that an AlSi7 alloy would be the optimal solution, reducing the amount of additional silicon needed to add to the recovered aluminium from the battery pack parts.

AlSi7 powder was produced by Vacuum Induction Melting Inert Gas Atomisation or VIGA and AlSi7Mg was produced by Centrifugal Atomisation. Vacuum Induction Melting Inert Gas Atomisation or VIGA is one of the leading powder manufacturing processes for the production of large quantities of spherical, high quality metal powders. VIGA is characterised by process reliability, good productivity and low operating costs and is a flexible, state-of-the-art production method. The VIGA system allows to consistently produce high quality spherical particles with low oxygen concentration. In addition, produced powders have high purity, good flowability and the possibility to define the particle size distributions (PSDs).

Figure 31 shows the VIGA atomiser available at CSIC installations. The VIGA system integrates a vacuum induction melting unit with an inert gas atomisation unit. The starting materials are melted by means of electromagnetic induction, where electrical energy is coupled into the crucible/material under vacuum or inert gas atmosphere. Once the desired melt homogeneity and chemical composition is achieved, the crucible is tilted into a gravity feeder. The fine metal stream flowing from the orifice of the melting funnel into the atomising nozzle system is subjected to a high-pressure jet of inert gas and then atomised. The combination of molten metal and gas jet creates a spray of micro-droplets which solidify in the atomisation tower to form a fine, spherical powder.

An appropriate proportion of the different pre-melted ingots were then mixed and atomised in a high-pressure gas atomiser with confined nozzle (Leybold VIGA 2S) at CSIC. Argon was used as the inert gas at a pressure of 22-25 bar. Accordingly, the atomiser crucible was loaded with 5 kg of aluminium, derived from the addition of 1,100 kg of AlSi20 mother alloy to 3,900 kg of ingots produced through the pre-melting of battery case components. The total weight of the argon atomised powder collected was 4,470 kg.



Figure 31. VIGA equipment used at the CSIC for the production of AlSi7 powder.

The production of powder by centrifugal atomization is achieved by melting material in a crucible and releasing it once it reaches its liquid state onto a metallic disc that rotates at high speeds. When the molten metal hits the spinning disc, it is atomized. Small particles are sprayed and projected from the disc into the surroundings where they are quickly cooled by contact with the inert gas inside the chamber. The process takes place in the atomizer, a sealed cone-shaped metal chamber housing an electric motor in Eurecat, as shown in Figure 32. This motor is responsible for rotating the disc attached to its shaft. The atomizer has two openings, one at the top and one at the bottom. In the upper part, there is a lid to which a cooled platform is attached, accommodating the induction coil surrounding the crucible. The lower lid houses the deposit that collects the atomized powder.

Based on the specific Si content and the quantity of each alloy, the resulting alloy weighed 11,94 kg and contained an average of 2,46% Si. To achieve the desired composition of the AlSi7Mg alloy with up to 7% Si, 1,26 kg of a 50%Al-50%Si master alloy was used to form the final AlSi7Mg alloy.



Figure 32. Centrifugal atomizer equipment used at Eurecat for the production of AlSi7Mg powder.

Figure 33 and Figure 34 depict the powder's morphology, which is predominantly spherical with a certain proportion of non-spherical forms and satellites. The atomized powder by both methods meets the requirements or qualities in morphology necessary for its use in additive manufacturing processes.



Figure 33. Scanning electron microscope image of the powder fraction $< 63 \mu\text{m}$ obtained from VIGA atomisation

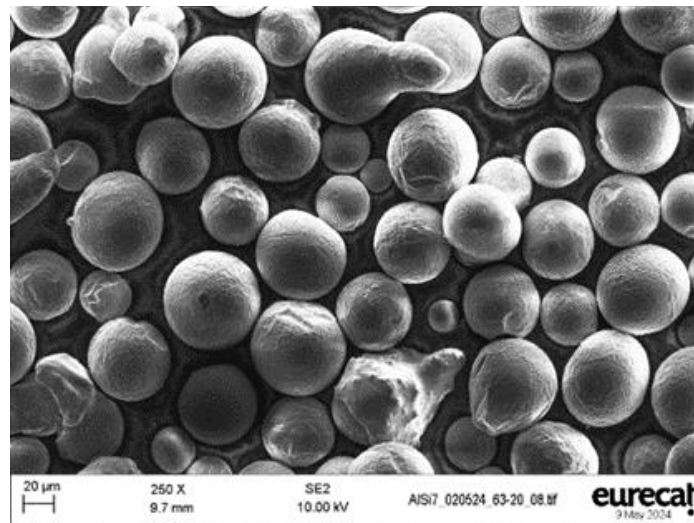


Figure 34. Scanning electron microscope image of the powder obtained from Centrifugal atomisation.

Copper powder was also produced by Centrifugal atomisation. Cut copper wire has been used as raw material. A total of 1.750 g of copper filaments were placed in a crucible made of graphite where they were melted by means of induction currents. The stopper which closes the outlet hole of the molten metal in the crucible is also made of graphite. The disc used was a flat disc with an alumina ceramic coating. Atomization was carried out at a speed of 35.000 rpm in an inert nitrogen environment. The disc during the atomization process was water-cooled to resist the molten copper which was heated up to 1.300°C. The Figure 35 shows SEM images of the copper powder with particles ranging from 45 to 75 µm. These images reveal a high degree of sphericity of the particles, with a smooth surface and barely any satellites.

8.1.3 Powder testing and optimisation for selective laser melting additive manufacturing

Selective Laser Melting SLM (or Powder Bed Laser Fusion) is an advanced additive manufacturing (AM) technology that enables the creation of high-precision metal parts. The process involves spreading a thin layer of metallic powder over a build platform and then using a high-powered laser to selectively melt and fuse the powder particles together, based on a digital 3D model. This process is repeated layer by layer until the entire object is formed. Figure 36 shows the SLM equipment available at CSIC and used for the 3D printing of the samples.

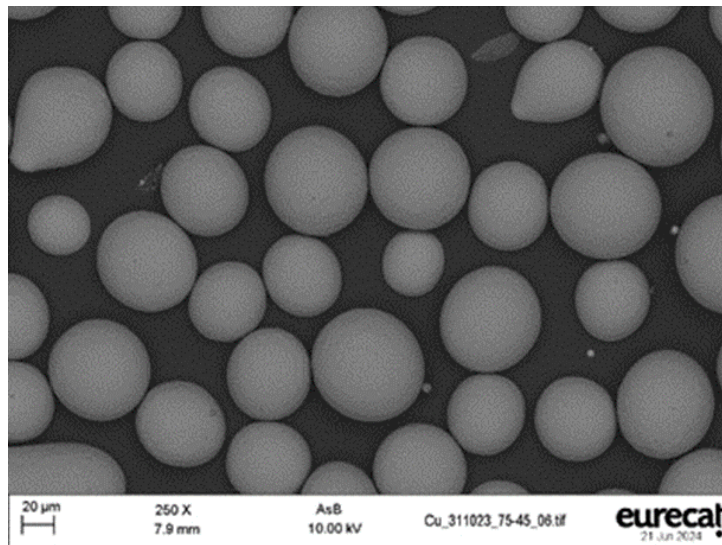


Figure 35. Scanning electron microscope image of the copper powder obtained from Centrifugal atomisation.

SLM is renowned for producing parts with excellent mechanical properties and high density, making it ideal for applications in aerospace, medical, automotive, and other industries where high strength and accuracy are essential. The technology allows for complex geometries that are difficult or impossible to achieve with traditional manufacturing methods, enabling innovative designs and lightweight structures. Selective Laser Melting (SLM) uses fine metallic powders as the primary material for building parts. As discussed previously, these powders are typically spherical in shape and with a uniform size distribution to ensure consistent layering and fusion during the SLM process.



Figure 36. SLM equipment available at CSIC

The fraction of the powder, both AlSi7 and AlSi7Mg, with a grain size below 63 μm was 3D printed using the SLM technique on a Renishaw AM250 with a laser power of 200W and a spot diameter of 70 μm . A protective atmosphere of argon with a maximum of 500 ppm O_2 was maintained throughout the fabrication of the samples to reduce oxidation during the melting process. A range of energy densities and laser scan speeds were evaluated to achieve the lowest porosity parts described below.

To evaluate the processability of this recycled AlSi7 powder for SLM, a two-level factorial design was employed, incorporating hatch point distance, exposure time and hatch distance. A layer thickness of 25 μm and laser power of 200 W were maintained consistently for all specimens. The samples of AlSi7 display remarkably high density across the entire range of values studied, with maximum values of 99.55% (porosity of 0.5%) and 99.98% (porosity of 0.02%). The samples of AlSi7Mg display also remarkably high density across the entire range of values studied, with values from 99.81% to 99.98% (porosity between 0.2% and 0.02%).

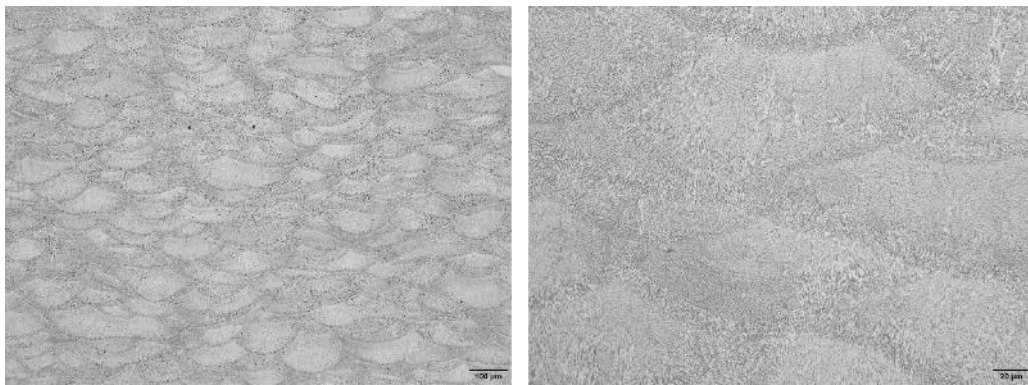


Figure 37. Optical microscopy microstructure of AlSi7 samples (x200 and x1000)

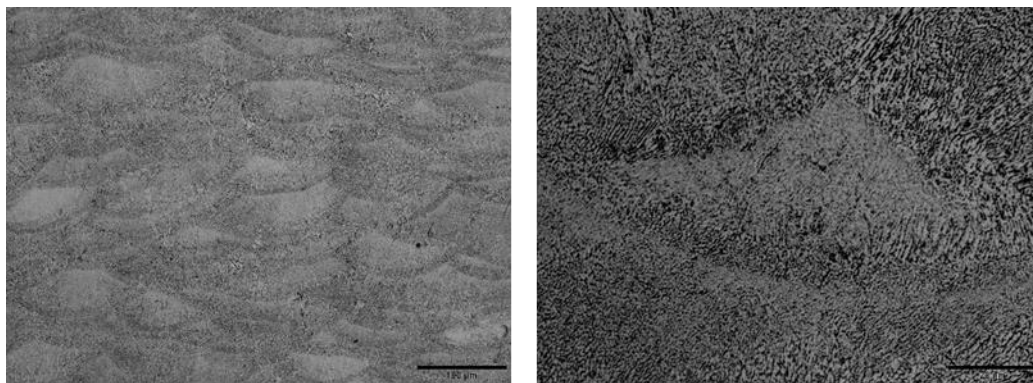


Figure 38. Optical microscopy microstructure of AlSi7Mg samples (x200 and x1000)

Figure 37 and Figure 38 show the typical microstructure of the AlSi7 and AlSi7Mg samples obtained by SLM. The microstructure is representative of the as-fabricated Al-Si alloys, exhibiting a fish scale-like morphology of molten

pools stacked layer by layer. The microstructure is composed of an α -Al solid solution and a network-like Si phase. The microstructure is consistent from sample to sample. However, there are two distinct zones in each melt pool. The core of the melt pool is characterised by a fine grain structure. At the edge of the pool a coarse dendritic microstructure can be seen with elongated and larger grains. As discussed previously the coarsening of the grains is caused by slower solidification at the boundary compared to the core.

The effect of the different composition of the aluminium alloy obtained by VIGA and centrifugal atomisation can be observed in the mechanical properties such as hardness. The average hardness of the AM samples of AlSi7 is 105 ± 5 (HV0.5) meanwhile the average hardness of the samples 3D printed with AlSi7Mg from centrifugal atomisation is 118 ± 6 (HV0.5). The value of AlSi7 is slightly lower than that of AlSi7Mg and reported AlSi10Mg obtained by SLM. The absence of Mg in this alloy means that the typical hardening of Al-Si-Mg alloys by solid diffusion of Mg in the Al matrix does not occur. This value is very close to the typical AlSi10Mg value obtained by other authors by SLM and remarkable higher to those of the AlSi10Mg obtained by high-pressure die casting (95–105 HV).

8.1.4 Results in powder production using centrifugal atomization

Details of the powder obtained, and its properties, are described in D3.5 Report on metal reuse as raw powder for Additive Manufacturing based on tasks carried out in T3.6. Recycling of metals at lab-scale. Figure 39 shows SEM images of AlSi7Mg and Cu powder using centrifugal atomization.

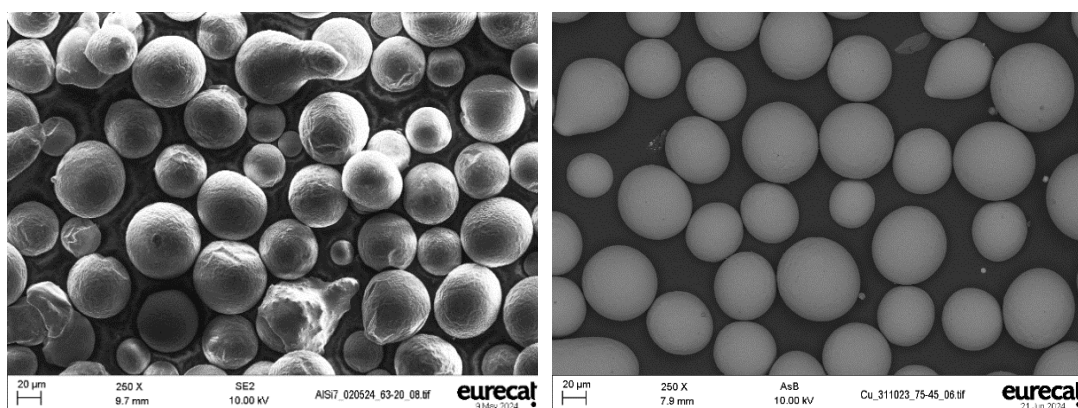


Figure 39: SEM images of AlSi7Mg powder (left) and Cu powder (right) obtained using centrifugal atomization in T3.6

To summarize, the quality obtained in AlSi7Mg and Cu powders fits the requirements of additive manufacturing processes. Both powders show spherical particles with a smooth outer surface and with no presence of satellites.

Also, the atomization of AlSi7Mg powders is a stable process and is demonstrated that the technology for this alloy can be scalable. However, for Cu powder more trials are required to get a stable atomization using recovered material from batteries. These trial tests will continue in Task T4.6 to study the scalability of processing recovered material.

8.2 Methodology to scale-up

A description of the atomization process is exposed in D3.5 Report on metal reuse as raw powder for Additive Manufacturing, in section 1.2.2 Atomizer description, to understand the challenges to overcome in this technology.

The main objectives to improve the capabilities and the readiness of the centrifugal atomization technology are:

1. Reduce median particle size of the powder obtained
2. Increase the capacity of the current pilot plant
3. Improve the operational aspects to reduce working times

To achieve these objectives the following tasks are proposed:

- Increase the maximum velocity of the disc: For this a revision of the current design is needed considering the vibration of the system during atomization.
- Increase crucible capacity: Redesign the crucible system of the current pilot plant.
- Increase the productivity of the pilot plant: Develop a control of the melt flow onto the disc to achieve a proper cooling of this component and maintain its integrity at long term.
- Reduce overall time for the atomization process: Improve some of the operational aspects of the current pilot plant, especially in the activities of powder collection after atomizing, and investigate how to reduce operating time of some tasks due to new component designs.
- Direct processing of metal scrap: Develop a device to use scrap metal directly to feed the centrifugal atomization pilot plant. Crushed metal with controlled size will be needed for this approach.

At this point of this project, on task T4.6. Scale-up for Metals recycling is proposed to start increasing the speed of the atomization disc, and next step will be increasing the crucible capacity and the control of the melt flow.

9. Synthesis of novel active materials

Along the FREE4LiB project, different routes for the production of novel cathode materials have been proposed and developed. On the one side, LUREDERRA is in charge of producing cathode materials with the Flame Spray Pyrolysis Technology (FSP); while on the other side, TORRECID is following processes based on solid state and hydrothermal routes.

On the following sections, both production routes are explained including main results obtained and the methodology to scale-up on the upcoming months of the project.

9.1 Synthesis of cathode materials by FSP

Main activity of LUREDERRA is to produce cathode materials on the Flame Spray Pyrolysis equipment (FSP) from recycled metal precursors. One important factor of this technology, is that the desired metals must be in an optimum liquid media, with specific physico-chemical properties (calorimetry, stability, and viscosity, among others). Thus, a transformation of the recycled materials received from partners into suitable precursor mixtures, is required. In that sense and for a good development of the activity, the process is divided into **two main stages**: the preparation of optimum recycled precursor mixtures for the FSP and the production of cathode materials on the FSP (Figure 40).

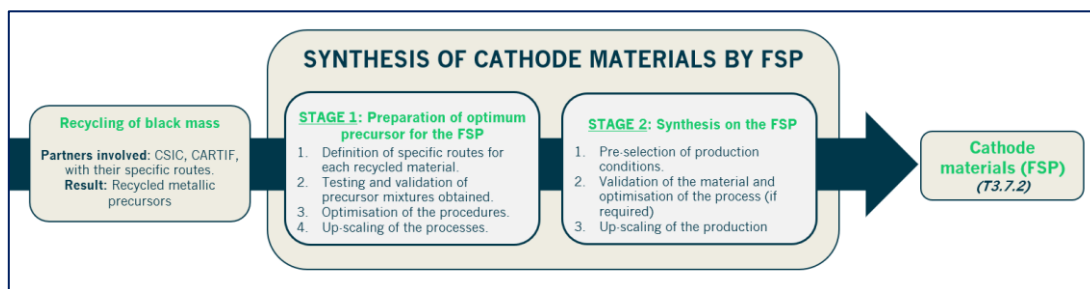


Figure 40. General overview of the process.

Stage 1: Production of optimum recycled precursor mixtures for the FSP.

This initial stage is covered on *Task 3.3* of the project, and *Deliverable 3.3* includes all the details concerning the different tests carried out with the recycled materials received from CSIC and CARTIF, the requirements that a precursor mixture might fulfil for a good compatibility with the FSP equipment and finally, some initial results and conclusions achieved.

Since the start of this task (T3.3.), several recycled precursors have been received from different partners (CSIC and CARTIF). Depending on the progress on the recycling of black mass, materials with different chemical natures were provided (oxides, carbonates, sulphates, oxalates...), as well as with different metal content. Considering the chemical behaviour of these materials, Lurederra defined specific routes to transform them into optimum liquid precursor mixtures for the later introduction into the FSP equipment. All the knowledge achieved, let Lurederra to define a general procedure for working with recycled materials (Figure 41).

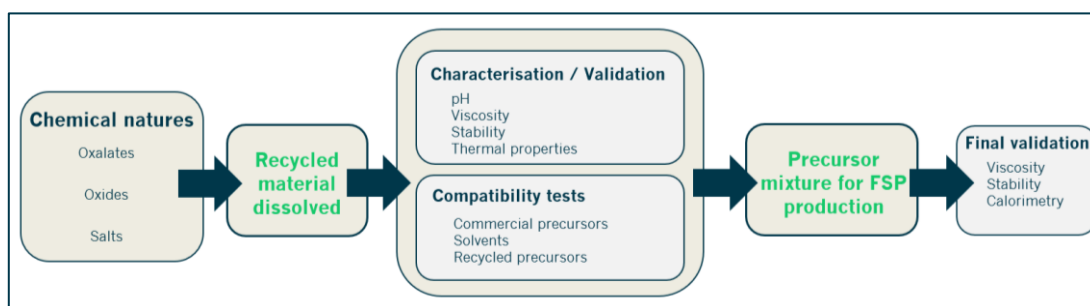


Figure 41. Procedure to transform recycled materials into optimum precursor mixtures.

Apart from the chemical nature of the materials, the metal content is another important factor to consider, as there are target cathode compositions to achieve. The pre-defined compositions in the project are NMC622, NMC811 and LiNMO, composed of nickel, manganese, cobalt, and lithium. It is important to clearly know the metal composition of the recycled material, to know if an enrichment is needed. As a source of enrichment, it would be possible to use both commercial and/or other recycled precursors.

On the following table (Table 21), a general overview of the recycled materials received from partners and the results obtained from them, are summarized.

Table 21. Overview of the transformation procedure to transform recycled materials into optimum precursor mixtures.

RECYCLED MATERIAL	METAL COMPOSITION	DESCRIPTION OF THE ROUTE FOLLOWED AND RESULT OBTAINED
Mixture of metal, metal oxides and graphite powder (CSIC)	Carbon, cobalt, nickel, manganese, and other impurities such as aluminium, iron and copper.	Firstly, a thermal treatment was required for the removal of graphite. Then, hard digestion conclusions were needed to transform the powder into a homogeneous solution. Nevertheless, due to the presence of different chemical natures on the powder, digestion tests resulted in inhomogeneous solutions.

Metal oxides (CARTIF)	Nickel, manganese, cobalt, lithium mainly.	The powder was directly dissolved in an acid media. The homogeneous digestion liquid was mixed with different solvents and a suitable precursor mixture for the FSP equipment was achieved including some pH adjustment.
Metal carbonates (CSIC)	Lithium	A liquid precursor was achieved directly from the carbonate, with the presence of an inorganic acid. Additionally, an intermediate salt was obtained from the carbonate to get a more-easily handled material. In both cases, a recycled precursor mixture was obtained.
Metal oxalates (CSIC)	Nickel, Manganese, Cobalt	A specific digestion procedure was defined and followed to get a homogeneous liquid solution without missing any interesting element on the process. The compatibility tests carried out after with different alcoholic media ended in good way, and a recycled precursor was achieved.
Sulphates (CSIC)	Cobalt	This material can be used directly as a cobalt precursor for enriching other precursor mixtures prepared with low quantity of this metal. It is compatible with an alcoholic media, after a pre-solution into water.

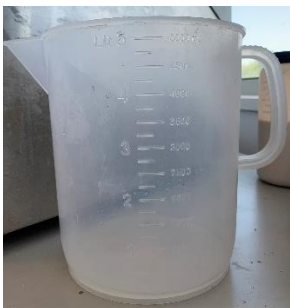






Analysing the results obtained and detailed on the above table (Table 21), the recycled materials pre-selected for the up-scaling are:

- Mixed metal oxides from CARTIF
- Lithium carbonate from CSIC
- Mixed oxalates from CSIC
- Cobalt sulphate from CSIC

For a good development of the up-scaling, Lurederra counts with equipment of different capacity for each of the stages of the transformation of recycled materials into optimum precursor mixtures (acid digestion, filtration, preparation of mixtures, and validation). This equipment includes reactors from 5 to 20L, stirring and mixing systems like shakers and stirring motors, different types of funnels, Büchner funnel for filtration and separation funnel for liquid-solid mixtures, several pumps to recirculate liquids, high-capacity beakers....

Following the same steps described in Table 22, Lurederra will adapt the procedures to the high-capacity equipment mentioned before.

Table 22. Equipment for the up-scaling.

STEPS	EQUIPMENT
Acid digestion (vessels, reactors, stirring motors...)	  
Filtration (Büchner funnel, pumps...)	 
Preparation and finetuning of the precursor mixture (reactors, stirring motors...)	 

Stage 2: Production of cathode materials on the FSP.

The activities included on this second stage are covered on *Task 3.7.2*, and preliminary results concerning the cathode powders produced are detailed on *Deliverable 3.6*.

The Flame Spray Pyrolysis technology is an innovative and industrially scalable process of synthesising a wide variety of metal oxide nanoparticles. The process consists of introducing a liquid precursor mixture into a combustion chamber through an atomizer, which disperse the mixture forming small droplets, which burn in the flame creating the nanoparticles. Main steps of the FSP equipment are identified on the following figure (Figure 42): injection of the precursor mixture, formation of the spray and combustion; and the collection of the material.

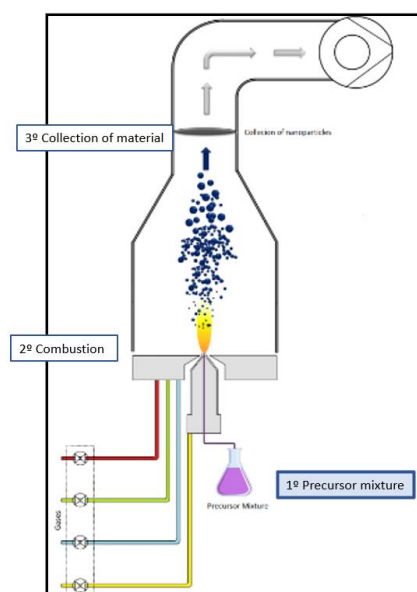


Figure 42. FSP equipment diagram with main stages: precursor mixture, combustion, and collection of material.

In each of these steps, specific parameters and configuration can be modified and adjusted depending on the requirements established. That is, those production parameters are key for getting the desired physico-chemical properties of the cathode material, and, crucial for the up-scaling of the process.

As mentioned at the beginning of this *Section 9.1*, the central point of this process is using recycled materials to synthesise cathode materials. Due to the complexity of the FSP process, initial productions have been carried out with commercial precursors, in order to identify possible critical points or aspects that would need an optimisation, before introducing recycled materials. In that sense and based on the pre-selected cathode compounds established on FREE4LiB project, LMNC, NMC622 and NMC811, Lurederra has produced several batches: NMC622, Li-NMC811 and an optimisation of this last composition. All these productions have been carried out in the laboratory scale FSP equipment (Figure 43, *left*), as only a few grams of cathode powder were enough for preliminary characterisation.

On the following table (Table 23), it is summarized the characterisation and properties of each of these cathode materials. The detailed characterisation is included in *Deliverable 3.6*.

Table 23. Cathode materials synthesised by FSP.

CATHODE MATERIAL PRODUCED	CHARACTERISATION
<p>CPO11 (NMC622)</p> 	<p>Surface Area = 36.5m²/g → Estimated particle size = 31.7nm</p> <p>Mass loss = 4.5 %</p> <p>SEM images = broader size distribution at the nanoscale to microscale</p> <p>EDS result = presence mainly of O, Ni, Co and Mn. Impurities of phosphorous due to using commercial precursors.</p> <p>XRD = crystalline mixed oxide phases (NiMn₂O₄, metallic Ni and Li_{1.85}Co_{0.815}O)</p> <p>Electrochemical performance = no specific capacity</p>
<p>CPO33 (LiNMC811)</p> 	<p>Surface Area = 53.8m²/g → Estimated particle size = 25.1nm</p> <p>Mass loss = 1 %</p> <p>SEM images = smaller particle size compared to CPO11 sample.</p> <p>EDS result = Mainly of O, Ni, Co and Mn; some impurities of Zn, P and Al.</p> <p>XRD = crystalline mixed oxide phases (Li₂CO₃, NiMn₂O₄ and Li_{1.85}Co_{0.815}O)</p> <p>Electrochemical performance = charge/discharge tests not conducted due to similarity with previous material</p>
<p>CPO44 (LiNMC811 low temperature production)</p> 	<p>Surface Area = 1.19m²/g → Estimated particle size = 1.13 μm</p> <p>XRD = identification of NMC811 crystalline phase</p>

Although, the production of cathode materials with good electrochemical behaviour is still on going, Lurederra has started defining the methodology to follow for the up-scaling.

The FSP technology is an industrially scalable process, and thus, Lurederra has several systems for manufacturing nanoparticles at different scales, having the capacity for productions from 10g/h (Figure 43, *left*), to pilot productions of 100g/h (Figure 43, *right*) and semi-industrial productions of 1 kg/h.



Figure 43. Left) Laboratory FSP equipment, 10g/h. Right) Pilot FSP equipment, 100g/h.

For the up-scaling, the production parameters validated and selected in the laboratory scale will be transferred to the pilot FSP equipment. The general structure of both equipment is similar, nevertheless, some adjustments will be required in order to achieve the same temperature conditions, which is a factor directly connected with how the nanoparticles are generated.

First parameters to adjust will be focused on the injection of the precursor mixture, looking for a stable and non-stop flame, which includes the flows of both precursor mixture and combustion gases. Then, the configuration of the nozzle and gas pressure will be essential to get a good atomization of the precursor mixture. And finally, the fan power, which will let us vary and move the heat inside the combustion chamber, as well as the particles, as desired.



Figure 44. Adjustment of parameters in FSP equipment

9.2 Synthesis of cathode materials through solid state and hydrothermal processes

9.2.1 Synthesis of active materials by solid state.

Within WP3, Task 3.7.1, TORRECID has evaluated diverse recycled materials described above, received as precursors for NMC622 and LNMO. The selected main technology was solid state synthesis since it allows high yield, low waste and is a cost-effective easy-scalable technology. For the evaluation of recycled lithium carbonate, a hybrid process using acetates was selected.

Solid state synthesis is based on reaction of raw materials starting from oxides or suitable raw materials like carbonates. The synthesis can be carried out within one step, or using two steps, with different holding temperatures and times, using partial or total mixture of raw materials by step. On the following table (Table 24), the recycled materials evaluated are listed.

Table 24. Recycled materials evaluated.

Sample	Details
BM01	Mixture of Ni, Mn, Co, C by hydrometallurgical process
BM02	Mixture of Ni, Mn, Co, C by hydrometallurgical process

BM01-LC	Lithium carbonate by hydrometallurgical process
PRE04	Mixture of Ni, Mn, by hydrometallurgical process
CP021	Mixture of Ni, Mn, Co, Li, Al, Cu by ultrasound delamination process

Once the structures were obtained, they were sent to IREC and Sakarya for analysis. Not all of them have been finished yet.

CP013 (FRN1-6) use of BMR01 in NMC622.

BMR01 was used in NMC622 synthesis. Due to low availability of precursors, 50% of material was used to reduce pristine raw materials. The synthesis was based on solid state. A first mixture of BMR01 and NiO, MnO₂ and CoO, was prepared, milled to 1 micron in wet, dried, and sintered at 950°C for 5 h. Afterwards the sintered mixed oxide was mixed with Li₂CO₃, milled again, and sintered again at 950 °C for 10 h.

Table 25. Used materials.

	Total materials used
CoO	8,07
NiO	24
MnO ₂	9,9
BMR01	42
Li ₂ CO ₃	39

The resulting powder was screened by 60 microns. XRD shows (Figure 45) main phase and an impurity of LiNiO (blue). This material was tested electrochemically but performance was not good due to high internal resistance.

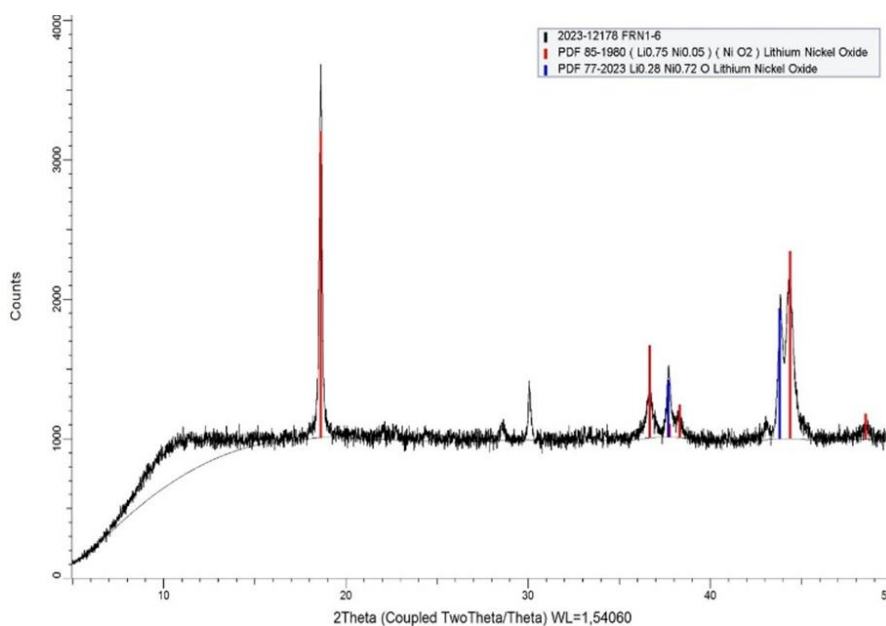


Figure 45. XRD of CP013.

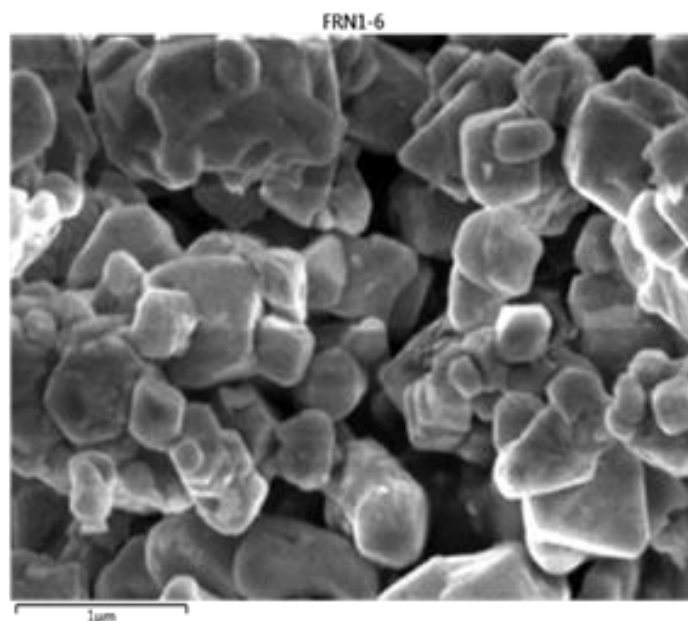


Figure 46. SEM image of CP013.

CP012 (FRL7) use of BMR02 in LNMO

BMR02 was used at 32 % in LNMO. Percentage was selected to keep cobalt content as low as possible in the LNMO. A twostep mixture was selected. First reaction of NiO and MnO₂ (addition of 32 % BMR01), milling to 1 micron in wet, drying and, synthesis at 900 °C 5 hours. Afterwards the powder was mixed with Li₂CO₃ in stoichiometric amount and a second treatment to perform lithiation at 800 °C 12 hours.

Table 26. Used materials.

	Total materials used
NiO	13,86
MnO ₂	47,52
BMRO2	32
Li ₂ CO ₃	21

XRD, represented on Figure 47, shows main LNMO phase and a small peak of contamination.

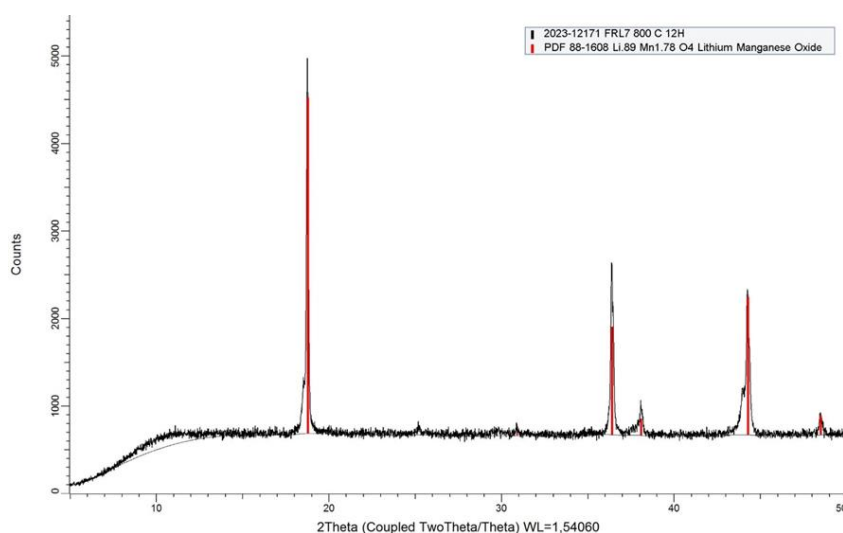


Figure 47. XRD CP012.

The sample did not show good electrochemical performance. Initial composition using pristine oxides provided 140 mAh/g specific capacity. Main reason could be presence of C and the difficulty in adjusting composition due to C presence.

CP014 (FRL8) use of recycled Li₂CO₃ in LNMO.

Hydrothermal process using acetates and Li₂CO₃ was selected for testing Li₂CO₃. Process was based on dissolution of acetates in water, drying at 80 °C for 24 hours and addition of recycled lithium source by milling. Finally thermal treatment was carried out at 800 °C for 20 hours. The XRD

Figure 48) shows a better structure compared to FRL-7. Main problem is the adjustment of Lithium.

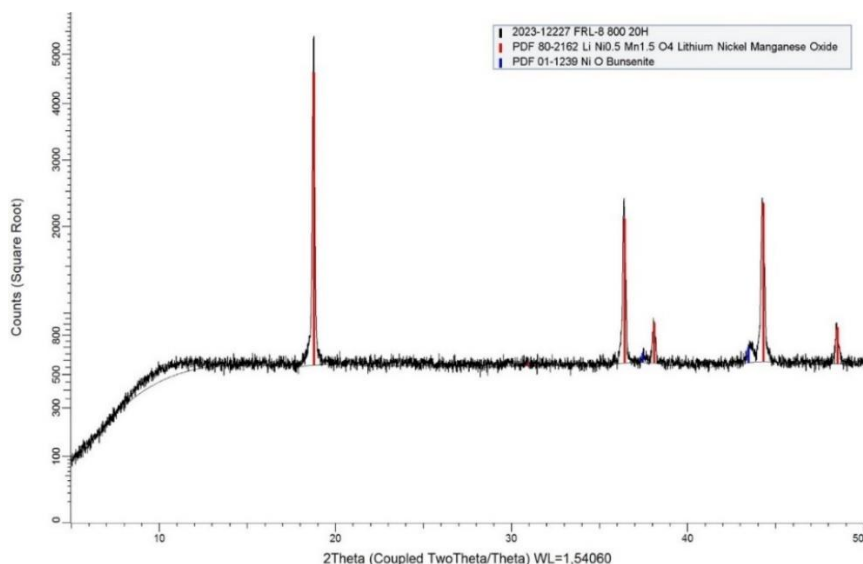


Figure 48. XRD of CP014

Material was characterized by IREC (electrode Active material (LMNO-CP0): 90%, Conductive material (super P): 5% Binder (PVDF): 5%) Cell set up Electrolyte: 1M LiPF₆ in EC: DEC 1:1 (by volume) (36 μ L/coin-cell) Separator: Celgard 2400 (single layer). Potential window: - 4.9 to 3.5 V As shown in Figure 49, performance is good, showing that recycled lithium carbonate can be used.

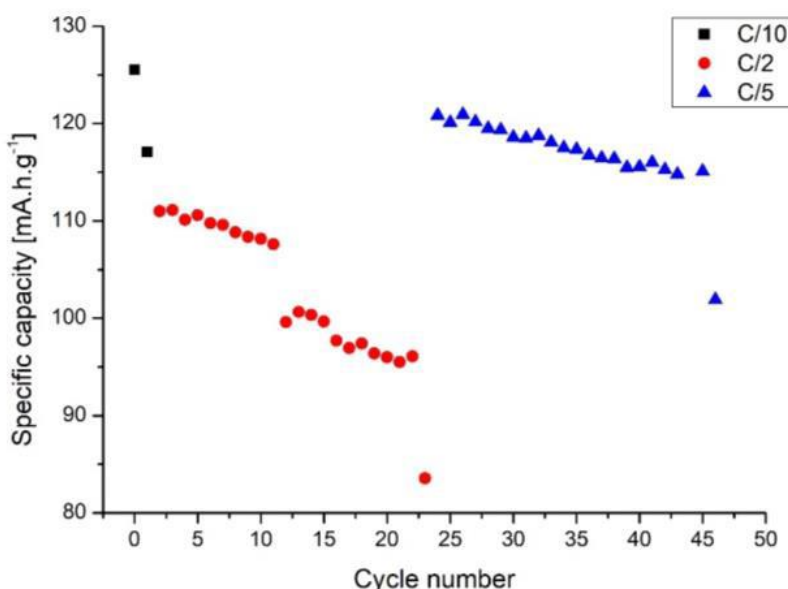


Figure 49. Specific capacity CP014.

CP021 is a black mass with presence of NiMnCoLi as well as Al and Cu. The material has a starting NMC like pattern. With CP021 the material was used in

direct synthesis replacing Ni, Mn, Co precursors as well as a lithiation step was performed.

Based on the analysis, NMC622 was prepared. Table 27 shows the different compositions evaluated.

Table 27. Compilation of compositions evaluated.

Samples	Details
CP024	(FRNC4) Lithiation of CP021
CP028	(FRNC1) 81 % reuse one step synthesis. Addition of Li, Ni, Mn, Co raw materials
CP025	(FRNC3) 89% use adjusting composition, Addition of Ni, Mn, Co raw materials
CP029	(FRNC5) 68% addition of Ni, Mn, Co, Li raw materials

As conclusion of the use of CP021 the product is feasible for production of NMC622. The results show good performance at levels of 68% of addition. It is important to highlight that one problem found is that although all samples were prepared adjusting the right composition of NMC622 all samples show defect in Ni.

Table 28. SEM-EDAX of samples.

% by SEM-EDAX	Ni	Mn	Co
std	54	8	3
CP024	47	11	13
CP028	40	16	15
CP025	40	15	14
CP029	47	19	17

CP024 (FRNC4)

CP021 was used as starting material for NMC622 carrying out a lithiation. Lithium is in excess in the structure coming from electrolyte. Thermal

treatment was performed to integrate the Lithium in excess into the ceramic network, Recrystallized CP021 was performed at 950 °C 10 h. XRD pattern is shown below (Figure 50). Lithium does not integrate in the structure, showing a non-right intensity peak ratio I19/I 43, ratio 0.66, showing bad mixing of Li and Ni.

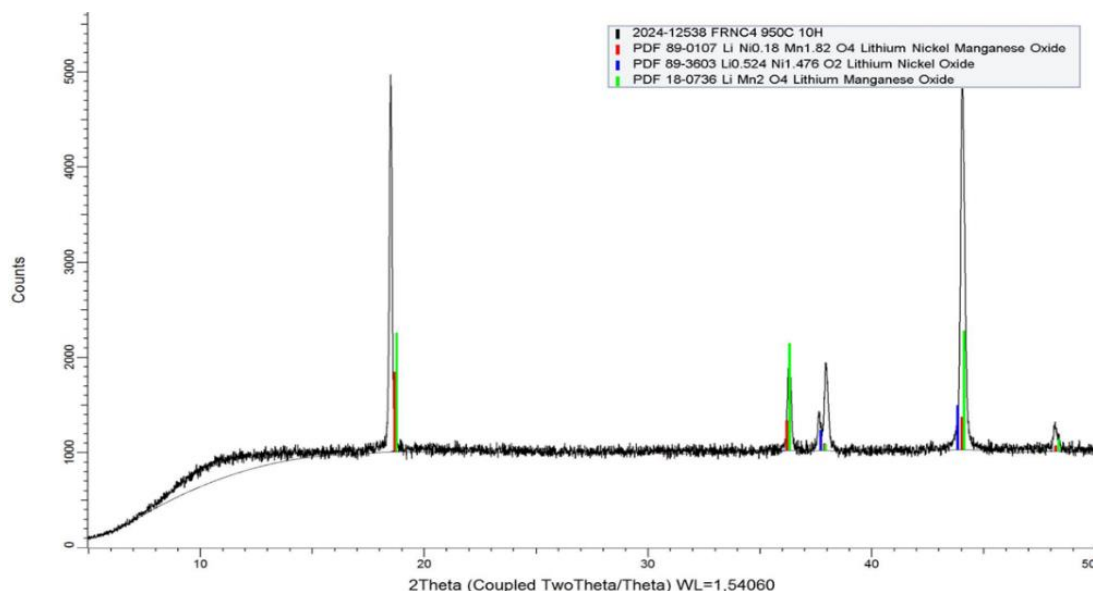


Figure 50. XRD of CP024.

Electrochemical tests showed bad performance.

CP028 (FRNC1)

NMC622 was prepared by testing a one-step synthesis process. Mixture of NiO, CoO, MnO₂, Li₂CO₃ and CP021 (81%) was prepared, CP021 was analyzed and the composition adjusted with oxides and Li₂CO₃ to achieve NMC622 composition. The mixture of raw materials was ball milled to 1 micron in wet, dried afterwards and sintered at 950 °C for 10 h. One step process was chosen since already part of structure is available. Composition of CP028 prepared is shown on the following table (Table 29).

Table 29. Composition of CPO28.

Raw material	%
CP021	81,0
NiO	0,4
MnO ₂	5,7

CoO	7,6
Li ₂ CO ₃	5,5

XRD pattern below (

Figure 51) shows a good crystallization without contaminating phases. Ratio of peaks I(19)/I(30) is low 1.13.

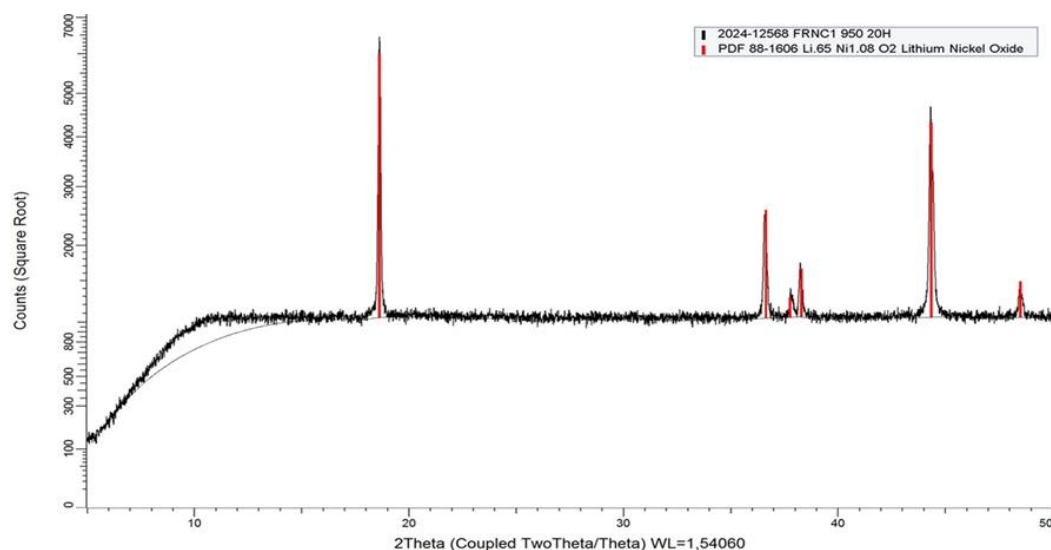


Figure 51. XRD CP028.

Electrochemical tests evaluated by IREC showed initial good specific capacity but decay quickly (Figure 52).

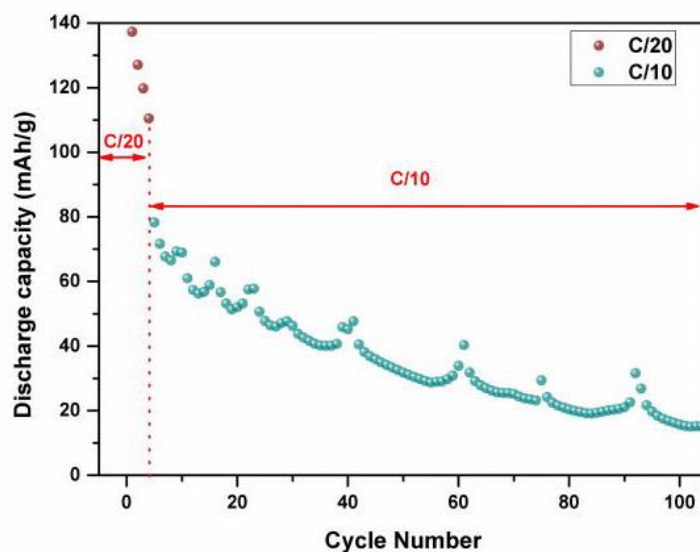


Figure 52. Specific capacity CP028.

CP025 (FRNC3)

NMC622 was prepared by testing one-step synthesis process. Mixture of CP021 and NiO, CoO and MnO₂ was prepared, CP021 was analyzed and the composition adjusted with oxides to achieve NMC622 composition. Use of CP21 was 89% The mixture was ball milled to 1 micron and sintered at 950 °C for 10 h. One step was chosen since part of structure is available. In this case no lithium was added. As can be seen in the XRD (Figure 53) by TORRECID by peak intensity, the lithiation is defect. Peak at 19 reflects the lithium intercalation, ratio of peaks I (19)/I (30) is 0.56 based on Sakarya measurement.

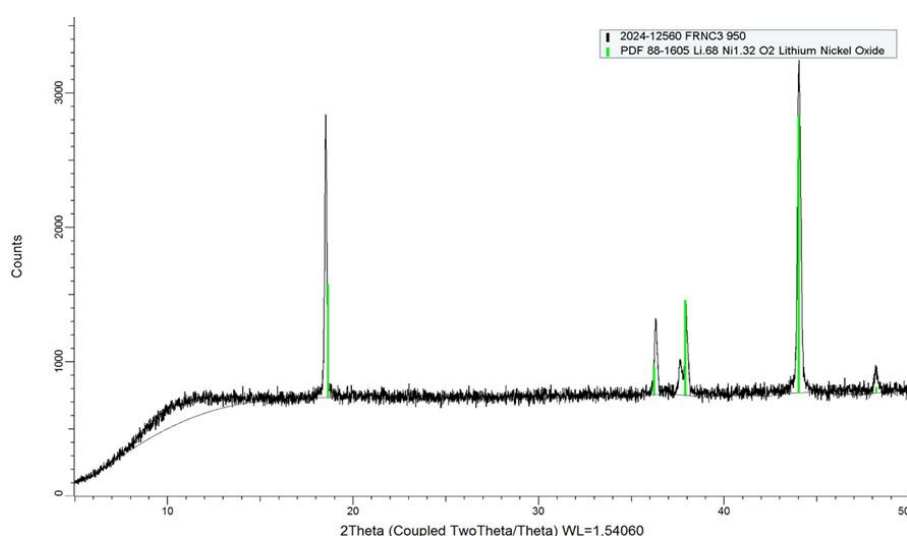


Figure 53. XRD CP25.

Electrochemical performance was bad (Figure 54).

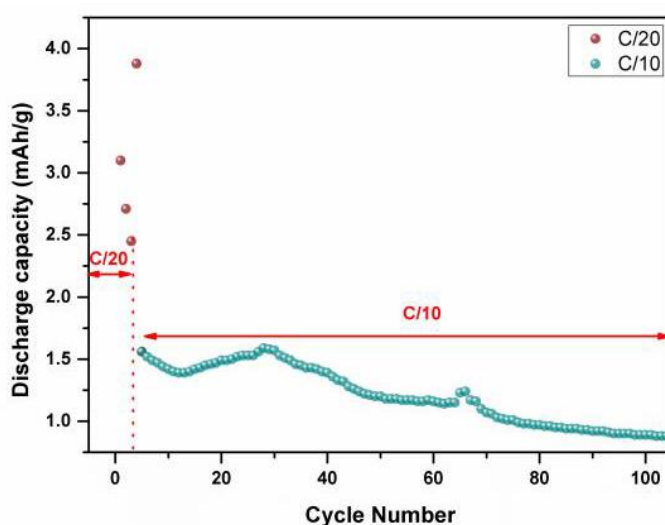


Figure 54. Specific capacity CP025.

CP029 (FRNC5)

NMC622 was prepared by testing one step synthesis process but at lower amount of CP021. Mixture of NiO, CoO, MnO₂, Li₂CO₃ and CP021 (68%) was prepared. CP021 was analyzed and the composition adjusted with oxides and Li₂CO₃ to achieve NMC622 composition. Raw materials were mixed, milled, and sintered. The mixture was ball milled to 1 micron and sintered at 950° C for 10 h. Intensity ratio of peaks I19/I30: 1.41 (Figure 55), showing good cation mixing. Table 30 shows the amounts used.

Table 30. Amount used.

Raw material	%
CP021	68,5
NiO	10,8
MnO ₂	4,5
CoO	5,4

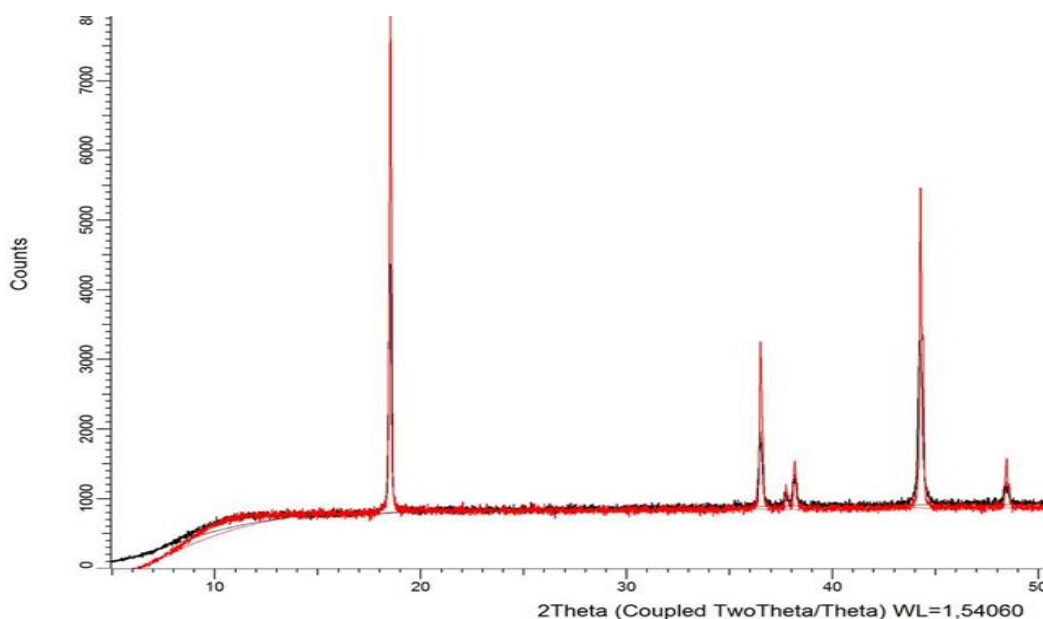


Figure 55. XRD of CP029.

CP029 was tested by Sakarya (Figure 56). Specific capacity is good, 140 to final 60 mAh/gr. Commercial NMC622 is in the range 160 to final 80 mAh/gr. Main difference is the particle size.

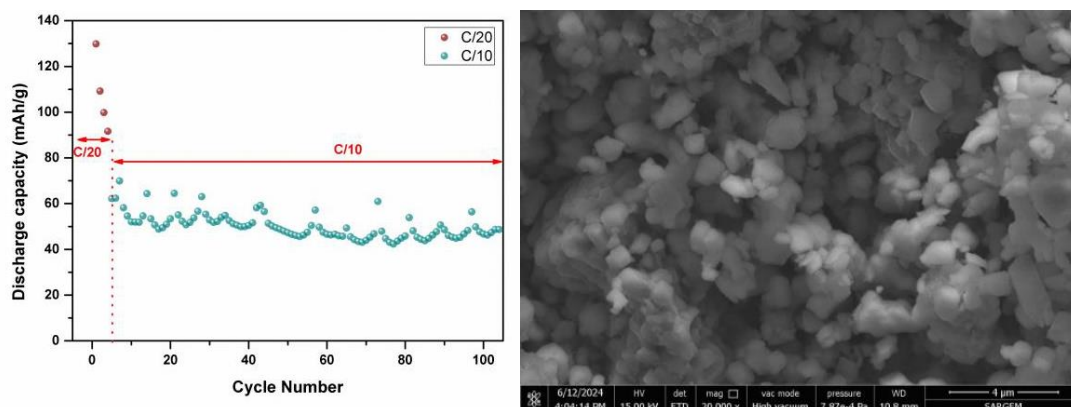


Figure 56. Specific capacity for CP029 and SEM image.

Use of PRE04

PRE04 was prepared by CSIC. It is a Ni-Mn-Li-Co mixture with low cobalt content. The powder was used as source for NMC 622 and LNMO.

CP037 FRN10

NMC622 was prepared by one step synthesis process. Mixture of PRE04 75 % and NiO, CoO, MnO₂ and, Li₂CO₃ to match NMC622 composition. The mixture was ball milled to 1 micron and sintered at 950° C for 10 h. XRD pattern (Figure 57) shows impurities of Ni_{0.8}MnO₂ as well as a defect of lithium in structure.

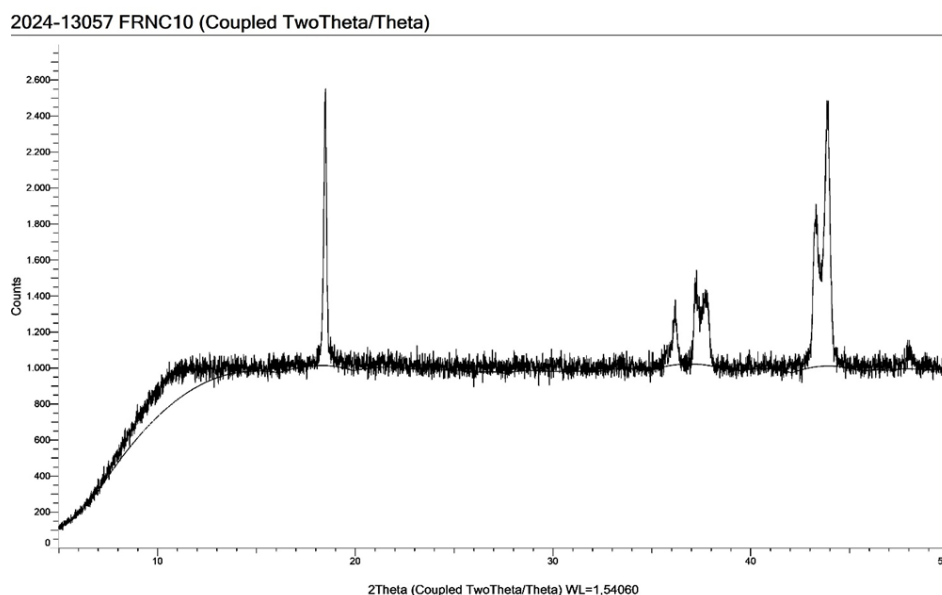


Figure 57. XRD CP037.

CP037 (FRNC9)

LNMO was prepared since PRE04 has a low cobalt content. A two-step mixture was selected. First reaction of NiO and MnO₂ with 50 % of PRE04, milling to 1 micron and, synthesis at 900 °C 5 hours. Afterwards mixture with Li₂CO₃ and second treatment for lithiation at 800 °C 12 hours. Table 31 shows overall composition.

Table 31. Overall composition.

Raw material	%
NiO	36
MnO ₂	13,4
PRE04	51.5
Li ₂ CO ₃	21.1

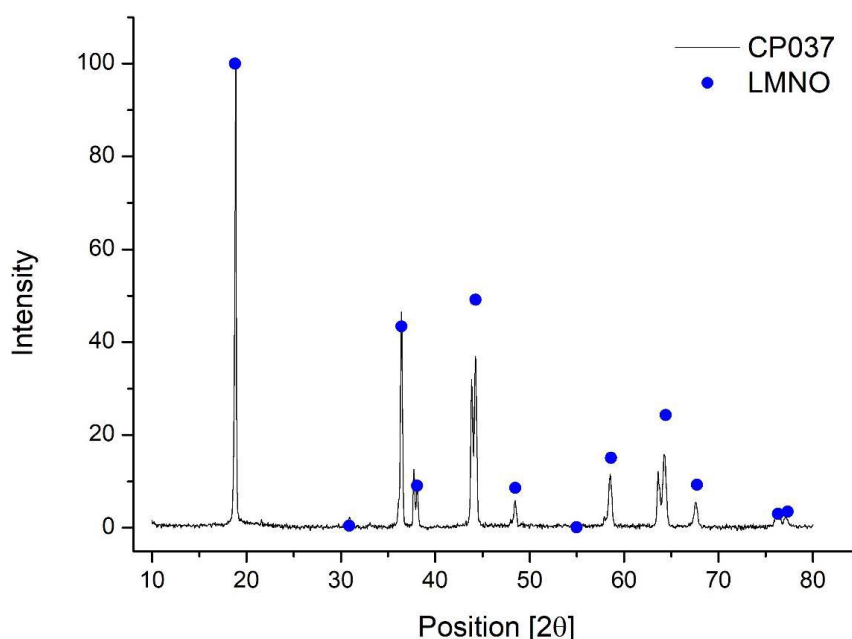


Figure 58. XRD CP37.

Sample was sent to IREC. In the case of electrochemistry performance the drop in capacity can be observed (Figure 59) as the cycles pass, starting with the first cycle with a capacity of 66.71 mA.h.g⁻¹ and ending with 23.83 mA.h.g⁻¹, giving an average in the 100 cycles of 35.14 mA.h.g⁻¹. Despite the impurities, the performance is about 50% of a commercial LNMO. Process can be optimized.

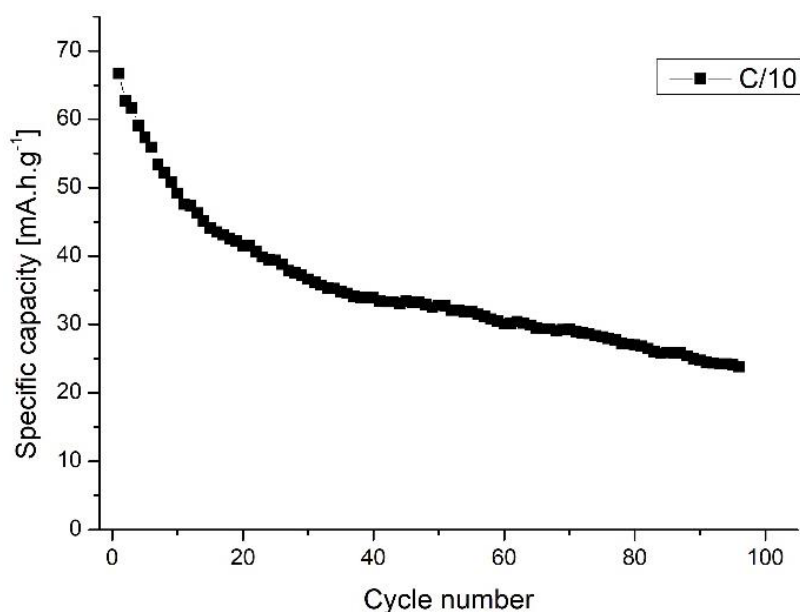


Figure 59. Specific capacity CP037.

XRD for standard LNMO is shown in Figure 60. As can be seen a second phase of $\text{Ni}_{0.8}\text{MnO}_2$ appears. It means that there is an excess of metals.

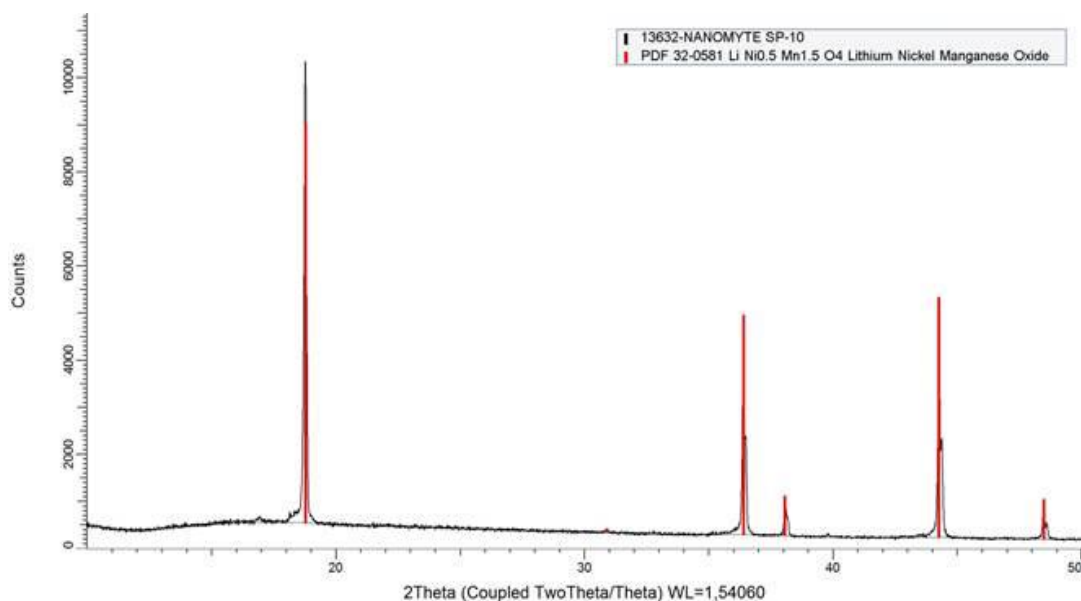


Figure 60. Reference LNMO XRD.

9.2.2 Methodology to scale-up

Based on results achieved by IREC and Sakarya university a methodology for industrial processing of materials have been identified. The methodology is important for future activities in WP4. It is important to highlight that an accurate analysis of samples is needed.

Solid state process for synthesis of NMC622, using CP021.

The use of CP021 enables to produce NMC622. Table 32 shows identified steps needed for the upscaling of process based on industrial capabilities.

Table 32. Methodology for the up-scaling.

Step	
Homogenization of CP021	Batch furnaces operate at average 4000 kg/batch. Homogenization of CP021 is required to get representative composition. 2720 kg have to be premixed.
Weighing of raw material composition	CP021 is mixed with NiO, CoO and Li ₂ CO ₃ .
Milling of composition	Mixture is pre-milled in mill in dry.
Sintering	Crucibles are loaded with powder and sintered at 900-920 °C for 8 hours.
Pre-crushing sintered pellets	The sintered powder is pre-milled to break agglomerates.
Jet milling	Powder is milled in dry by jet milling to 10micron size.
Packing	Powder is packed in sealed bags.

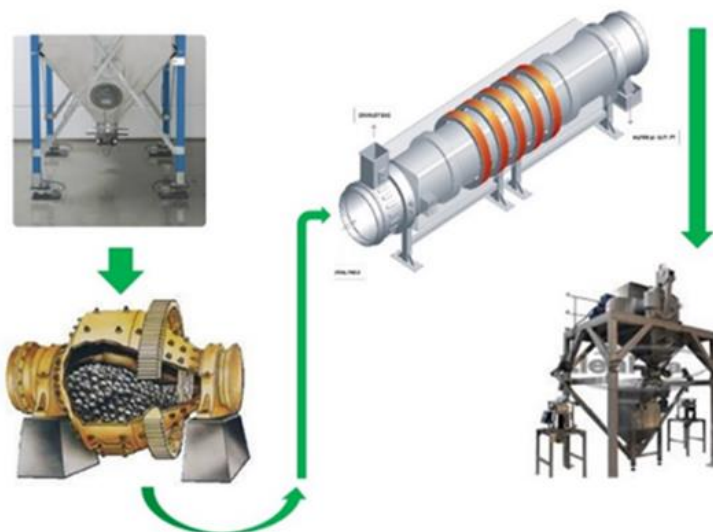


Figure 22. Process: weighing, milling (wet or dry), sintering, jet milling.

Solid state process for synthesis of LNMO, using PRE04 type.

The use of PRE04 type precursors enables to produce LNMO. Process can be applied to any mixture type PRE04 with different analysis. Main problem identified is the right analysis to adjust. Table 33 shows identified steps needed for the upscaling of process based on industrial capabilities.

Table 33. Methodology for the up-scaling.

Step	
Homogenization of PRE04	Batch furnaces operate at average 4000 kg/batch. Homogenization of PRE04 is required to get representative composition 2040 kg.
Weighing of raw material composition	PRE04 is mixed with NiO, MnO ₂ . NiO 36 MnO ₂ 13 PRE0451
Milling of composition	Mixture is pre-milled in mill in dry.
Sintering	Crucibles are loaded with powder and sintered at 900 5 h.
Mixing	NiMnO is mixed with Li ₂ CO ₃ .
Milling	Dry milling.
Sintering	Sintering 800 °C 12 h.
Pre-crushing sintered pellets	The sintered powder is pre-milled to break agglomerates.
Jet milling	Powder is milled in dry by jet milling to 10micron size.
Packing	Powder is packed in sealed bags.

10. Cell manufacturing research

The methodology to scale-up cell manufacturing research will be included in D3.6 “Report on validation of recovered materials re-use on new cells” due to a slight delay in the results.



11. Study of recovery materials harnessing in other fields

11.1 Results

Results of performance and integration of recycled material in other fields like ceramic pigments and frits are reported in D3.9

11.2 Methodology to scale-up

Black mass and recycled precursors can be used either in ceramic pigments or in frits for enamels.

D.39 summarize the test carried out based on suitability of tested materials.

In the case of ceramic pigments, ceramic pigments are suitable as host to integrate diverse mixtures as demonstrated with CP021. For the upscaling of pigment preparation, focusing on black pigments, using Ni and Co, Table 34 shows the methodology.

Table 34. Methodology to scale-up pigment preparation

STEP	
Homogenization of recycled material	Batch furnaces operate at average 4000 kg/batch. Homogenization is required to get representative composition.
Weighing of raw material composition	Mixing of recycled material with other oxides: CoO, Fe ₂ O ₃ , MnO ₂ , CoO
Milling of composition	Mixture is pre-milled in mill in dry.
Sintering	Crucibles are loaded with powder and sintered at 1200-1300 °C
Pre-crushing sintered pellets	The sintered powder is pre-milled to break agglomerates
Jet milling	Powder is milled in dry by jet milling to 10 micron size
Packing	

In the case of use in Frits for enamels, the amount is lower, since metal are about 4 % in composition (Table 35).

Table 35. Methodology to scale-up frits preparation

STEP	
Homogenization of recycled material	Batch furnaces operate at average 1000 kg/batch. Homogenization is required to get representative composition. In the case of continuous furnaces it is much more important
Weighing of raw material composition for frit	Minoritary elements (< 4 %) are added separately to not contaminate hydraulic feeding
Mixing	Raw materials are mixed in high-speed mixer
Melting	Frit is molten in continuous furnaces or batch furnaces between 1300 and 1400 °C. After melting frit is water quenched.
Packing	

12. Conclusions

This document collects the technologies that will be scale-up during WP4. All the results here collected seems to be very promising for the consecution of the validation of at least 8 technologies as stated in the GA. The technologies that will be scaled are:

- robot assisted dismantling (tech #1),
- pre-treatment, including mechanical, electrohydraulic fragmentation, and non-breaking delamination (techs #2a, #2b and #2c)
- recovery of metals from black mass (using a combination of tech #4a and #4b)
- cathode direct recycling (techs #3b and #3c)
- recycling of plastics (techs #5a and #5b)
- recycling of metals (techs #7a, #7b and #6)
- active materials synthesis based on recycled precursors (techs #8a, #8b and #8c)
- material re-use on new pouch cell production (tech #9c)

The investigation into robotic disassembly of EV batteries showcases the potential for significant advancements in efficiency, safety, and environmental impact. By employing robotic systems to handle the disassembly process, it is possible to achieve higher precision and repeatability. Moving forward, the focus will be on refining the developed technologies and scaling them to meet industrial demands, demonstrating the readiness level of robotic systems for battery recycling operations.

The treatment of battery cells with electrohydraulic fragmentation is an innovative method with a completely new approach. In contrast to other processes, the battery cells are shredded and separated with shock waves almost exclusively under water. On pilot scale the EHF process is comparable to well-known or standard processes and presents similar key figures. Though up-scaling appears to be more demanding compared to other dry procedures due to the basic requirements. The launch of the continuous system in autumn will provide sufficient data.

To effectively recover each metal from the black masses, CSIC will scale up the most promising technology based on laboratory-scale results. Two different black masses from a thermo-mechanical pre-treatment process from ACCURREC (BM01), and come from an electrohydraulic fragmentation process from FRAUNHOFER (BM03) will be assessed. A combined pyro-hydrometallurgical process will be selected for this purpose. If needed, CSIC will optimize experimental conditions to improve the recovery process. Several precursors will be obtained, including lithium carbonate, nickel, manganese and cobalt oxalate, nickel and manganese chlorides/oxalates, as well as cobalt sulphate. , that will be used as raw materials for the production of cathode materials.

As detailed in Section 9. Both partners, LUREDERRA and TORRECID, will continue producing cathode materials based on their technologies, and selecting the materials more promising for the up-scaling. In terms of the up-scaling, a preliminary methodology has already been defined, nevertheless, optimisations and modifications will be carried out in case it is required.

Results achieved reported in D3.8 have validated initial revalorization of recycled precursors and black mass in novel active materials NMC622 and LNMO, 68 % of black mass mixture and 50% of precursor mixture shown the capability to reduce pristine materials and validate processing carried out in tasks 3.3. Deliverables has defined industrial process for upscaling cathode production. Results allows to advance Free4lib within ST02 “develop until TRL3-TRL4 8 innovative technologies for recovered materials re using and explore options to harness non reusable elements in other fields”.

Direct recycling technologies are giving promising results from the laboratory scale although it is soon to start thinking on its feasibility in an industrial

environment, the next years of implementation and scaling-up of them will be key to develop further process and exploit these solutions in future projects or contracts with stakeholders.

Recovery of plastic components after EV battery pack dismantling allows the proper recycling of plastic materials. The identification methods based on optical analysis (NIR and FTIR spectroscopy) have led to the identification of the different polymer types used in the manufacturing of EV battery plastic components. Definition of the most feasible case studies for EV battery plastic components recycling has been made considering material source availability and suitability for upscaling operations. For each case study the benchmarking polymer types and grades have been set according to product performance requirements. Laboratory tests have been performed at laboratory level for materials properties characterization using test specimens manufactured with corresponding thermoplastic granulates and pellets. Results from laboratory tests suggest that service conditions have led to some downgrading in plastic components and losses in the material properties performance.

Overall, the outcomes obtained from each case study will set the basis for reprocessing and upcycling methodology of the recovered plastic materials in further *WP4 Task 4.5 Scale-up for plastic materials recycling*, with the aim of obtaining thermoplastic compounds formulated with recycled content for their reuse in battery plastic parts or other high value applications.

A battery pack case was disassembled into its constituent components, and the different aluminium alloys present were identified as AlSi12, 5xxx, 3xxx and 6xxx series. The alloys were successfully grouped, melted and remixed to form an AlSi7 alloy, targeted and suitable for SLM.

The production of powder by Inert Gas Atomization of the recycled aluminium resulted in a powder with a particle size distribution appropriate for SLM, particularly in the < 63 µm range. The morphology was predominantly spherical and the internal structure was free of significant pores, indicating that the material is of a quality appropriate for AM purposes.

The production of AlSi7 powder by Centrifugal Atomization of the recycled aluminium resulted in powder suitable for additive manufacturing processes. obtaining spherical powder without satellites. For Cu powder production extra tests using recovered metal are required to set-up the technology, although powder obtained for initial tests are suitable for additive manufacturing.

A factorial design study identified the optimal SLM parameters to minimise porosity and achieve densities above 99.9% using both powders produced by VIGA Atomisation and Centrifugal Atomisation. The optimum requires a slightly higher energy density than that of used for commercial AlSi10Mg powders but

all the range of energy density and scan laser speed offer a superb density. In other words, the SLM process has proven to be very robust around this optimum for the production of fully dense parts.

In both cases the atomised powder was sieved and only the $< 63 \mu\text{m}$ range was used and no statistical significance differences was observed in the resulting sample density with SLM optimum parameters.

The composition of the obtained parts reveals a higher proportion of Fe than that observed in SLM parts made from commercial powder. However, the as-built microstructure of the printed AlSi7 alloy demonstrated typical fine microstructures with distinct melt pool boundaries and the absence of detrimental AlSiFe precipitates. The mechanical testing demonstrated that the hardness values ($105 \pm 5 \text{ HV}$) with powder of AlSi7 were slightly lower than those of AlSi10Mg due to the absence of magnesium, but the hardness obtained with powder of composition AlSi7Mg ($118 \pm 6 \text{ HV}$) increases. The ultimate tensile strength and % elongation values were within the range of those typically observed in SLM-produced AlSi alloys. Further work is required to investigate the evolution of these alloys rich in Fe impurities during heat treatments to improve their ductility.

The results confirm the feasibility of using recycled aluminium from EV battery packs for high quality AM applications. This approach not only provides a sustainable method of reusing valuable materials, but also reduces the environmental impact associated with primary aluminium production.